

See discussions, stats, and author profiles for this publication at: <https://www.researchgate.net/publication/335002027>

Lessons learned implementing an operational continuous United States national land change monitoring capability: The Land Change Monitoring, Assessment, and Project (LCMAP) approach...

Preprint in Remote Sensing of Environment · August 2019

DOI: 10.1016/j.rse.2019.111356

CITATIONS

27

READS

1,607

21 authors, including:



Jesslyn F. Brown

United States Geological Survey

131 PUBLICATIONS 9,018 CITATIONS

SEE PROFILE



Qiang Zhou

United States Geological Survey

11 PUBLICATIONS 99 CITATIONS

SEE PROFILE



John L. Dwyer

United States Geological Survey

32 PUBLICATIONS 1,955 CITATIONS

SEE PROFILE



Jim Vogelmann

United States Geological Survey

82 PUBLICATIONS 9,590 CITATIONS

SEE PROFILE

Some of the authors of this publication are also working on these related projects:



Mapping and Characterizing Human Activity Changes using NASA Black Marble Product Suite [View project](#)



Dynamics and sustainability of the global savanna and grassland biomes [View project](#)



ELSEVIER

Contents lists available at ScienceDirect

Remote Sensing of Environment

journal homepage: www.elsevier.com/locate/rse

Lessons learned implementing an operational continuous United States national land change monitoring capability: The Land Change Monitoring, Assessment, and Projection (LCMAP) approach

Jesslyn F. Brown^{a,*}, Heather J. Tollerud^a, Christopher P. Barber^a, Qiang Zhou^b, John L. Dwyer^a, James E. Vogelmann^a, Thomas R. Loveland^a, Curtis E. Woodcock^c, Stephen V. Stehman^d, Zhe Zhu^e, Bruce W. Pengra^f, Kelcy Smith^f, Josephine A. Horton^g, George Xian^a, Roger F. Auch^a, Terry L. Sohl^a, Kristi L. Sayler^a, Alisa L. Gallant^a, Daniel Zelenak^g, Ryan R. Reker^f, Jennifer Rover^a

^a U.S. Geological Survey (USGS), Earth Resources Observation and Science (EROS) Center, 47914 252nd Street, Sioux Falls, SD 57198, USA

^b ASRC Federal Data Solutions, Contractor to the U.S. Geological Survey, Earth Resources Observation and Science (EROS) Center, 47914 252nd Street, Sioux Falls, SD 57198, USA

^c Department of Earth and Environment, Boston University, 685 Commonwealth Avenue, Boston, MA 02215, USA

^d Department of Forest and Natural Resource Management, State University of New York, Syracuse, NY 13210, USA

^e Department of Natural Resources and the Environment, University of Connecticut, Storrs, CT 06269, USA

^f KBR, Contractor to the U.S. Geological Survey, Earth Resources Observation and Science (EROS) Center, 47914 252nd Street, Sioux Falls, SD 57198, USA

^g Innovate! Inc., Contractor to the U.S. Geological Survey, Earth Resources Observation and Science (EROS) Center, 47914 252nd Street, Sioux Falls, SD 57198, USA

ARTICLE INFO

Keywords:

Time series
Landsat
Analysis Ready Data
Land cover
Change detection
Monitoring
Earth observations

ABSTRACT

Growing demands for temporally specific information on land surface change are fueling a new generation of maps and statistics that can contribute to understanding geographic and temporal patterns of change across large regions, provide input into a wide range of environmental modeling studies, clarify the drivers of change, and provide more timely information for land managers. To meet these needs, the U.S. Geological Survey has implemented a capability to monitor land surface change called the Land Change Monitoring, Assessment, and Projection (LCMAP) initiative. This paper describes the methodological foundations and lessons learned during development and testing of the LCMAP approach. Testing and evaluation of a suite of 10 annual land cover and land surface change data sets over six diverse study areas across the United States revealed good agreement with other published maps (overall agreement ranged from 73% to 87%) as well as several challenges that needed to be addressed to meet the goals of robust, repeatable, and geographically consistent monitoring results from the Continuous Change Detection and Classification (CCDC) algorithm. First, the high spatial and temporal variability of observational frequency led to differences in the number of changes identified, so CCDC was modified such that change detection is dependent on observational frequency. Second, the CCDC classification methodology was modified to improve its ability to characterize gradual land surface changes. Third, modifications were made to the classification element of CCDC to improve the representativeness of training data, which necessitated replacing the random forest algorithm with a boosted decision tree. Following these modifications, assessment of prototype Version 1 LCMAP results showed improvements in overall agreement (ranging from 85% to 90%).

1. Introduction

Humans have modified the Earth's surface for millennia, but only recently has a formal, interdisciplinary land change science emerged as a consequential field of study (Turner et al., 2007). Improvements in sensor technologies, spatial tools, computing resources, and algorithm

development have all helped to advance the science. There has also been the realization of the importance of the topic to science and society. The National Research Council (2001) identified land change dynamics as one of the seven grand challenges in environmental science. In an evaluation of millennium ecosystem assessment needs, the lack of global time series information on land cover change is

* Corresponding author.

E-mail address: jfbrown@usgs.gov (J.F. Brown).

<https://doi.org/10.1016/j.rse.2019.111356>

Received 18 September 2018; Received in revised form 26 July 2019; Accepted 31 July 2019

0034-4257/ Published by Elsevier Inc.

considered particularly constraining for meeting the needs of decision-makers for scientific information on the consequences of ecosystem change (Carpenter et al., 2006). As a result, understanding land use and land cover change has become an important theme in global change, climate change, Earth systems, and ecosystem sustainability research programs (Gutman et al., 2004). Turner et al. (2007) advocated for advancing land change science for multiple applications, with a strong emphasis on improving land observation and monitoring.

The specific applications of land cover change information are many and varied. Land cover change information has been used to assess anthropogenic release of CO₂ to the atmosphere (Achard et al., 2004; Houghton et al., 2012); assess carbon stocks and sequestration potential (Wu et al., 2015; Tan et al., 2015); model changes in hydrologic dynamics in natural and agricultural ecosystems (Stow et al., 2004; Senay et al., 2016); monitor fires and fire fuel (Eva and Lambin, 2000; Rollins, 2009), forest disturbance/deforestation (Masek et al., 2008; Hansen et al., 2013; Kennedy et al., 2014), and urbanization (Fu and Weng, 2016); model historical and future land cover (Sleeter et al., 2012; Sohl et al., 2012; Sohl et al., 2016); and measure and evaluate changes in vegetation phenology (Melaas et al., 2013; Zhou et al., 2016; Li et al., 2017). It is important that we develop a better breadth of knowledge about the rates, types, causes, and consequences of the changes taking place so that scientists, resource managers, and other decision makers can respond appropriately.

Remote sensing is well suited for characterizing land cover change information and is appropriate for assessing land changes from local to global scales. With the advance of technology and decreasing satellite data cost, various regional and global land cover mapping products have been produced. The U.S. Geological Survey (USGS) has a long history of using moderate spatial resolution remote sensing data (including Landsat, Moderate Resolution Imaging Spectroradiometer, and Advanced Very High Resolution Radiometer) to characterize landscape change to support regional and national assessments for both science and management regarding the extent, location, magnitude, impact, and trajectory of land cover change. The USGS National Land Cover Database (NLCD) has produced 30 m land cover products derived from Landsat data since 1992 (Vogelmann et al., 1998; Fry et al., 2011; Xian et al., 2011; Homer et al., 2015). Currently, NLCD is updated every 5 years for the conterminous United States (CONUS) and every 10 years for Alaska. The NLCD has provided data historically linked to a specific year but has not been updated annually.

The USGS Land Cover Trends (Trends) project used Landsat data to provide land cover status and trends information at regular time intervals from 1973 to 2000 across CONUS (Loveland et al., 2002; Sleeter et al., 2013). These products have been widely used for a variety of research and applications (Liu et al., 2004; Hale et al., 2008; Barnes and Roy, 2010; Soular and Wilson, 2015; Sohl et al., 2016). Similarly, other monitoring efforts in Canada (Latifovic and Pouliot, 2005; Olthof et al., 2015), Brazil (Macedo et al., 2013; IBGE, 2018; INPE, 2018), India (Roy et al., 2008), Australia (Lymburner et al., 2013), China (Deng and Liu, 2012; Hu et al., 2014), Europe (Feranec et al., 2016; Inglada et al., 2017), and Russia (Schepaschenko et al., 2011) have also produced land cover datasets using moderate spatial resolution imagery.

Systematic large area land cover monitoring became prevalent in recent years after Landsat data were made available free of charge by the USGS (Hansen and Loveland, 2012; Hansen et al., 2014). The ready access to the rich Landsat image archive has created new opportunities for characterizing land cover change at more frequent time intervals than previously possible. Increased spatial, spectral, and temporal resolutions provide numerous opportunities to make substantial advances in understanding our changing planet. A number of methods for detecting change at an annual time interval have utilized substantial data volumes (Huang et al., 2010; Kennedy et al., 2010; Vogelmann et al., 2012; Hughes et al., 2017). Approaches that utilize a time series of all observations to detect change at each observation have also been

developed (Verbesselt et al., 2012; Brooks et al., 2014; Zhu and Woodcock, 2014). The use of time series metrics for land change detection and change characterization can increase information content, minimize data noise prior to classification, and improve classification accuracy (Zhu and Woodcock, 2014; Wulder et al., 2018).

As discussed by Wulder et al. (2018), the field of land cover monitoring has improved dramatically over the previous four decades, with computer software and hardware systems increasing the capacity to analyze large volumes of data for science and applications. Wulder et al. (2018) conclude that efficiencies in information generation will result in multiple different land cover products, thus requiring well-calibrated input imagery, well-understood algorithms, and rigorous accuracy assessment protocols. Although efforts exist that provide land cover information with improvements in spatial, spectral, thematic, or temporal information (Hansen et al., 2013; Yan et al., 2015; Hermosilla et al., 2018; Song et al., 2018), few approaches have reached a level of maturity to: (1) become operational with annual temporal time steps at the Landsat spatial scale, (2) cover national to global areas, (3) provide thematic coverage of all land cover sectors (e.g. some prior efforts may produce results for forested landscapes alone), and (4) provide statistically based estimates of rates of land surface change and their uncertainties.

In this paper, we present the foundational elements and lessons learned implementing the Land Change Monitoring, Assessment, and Projection (LCMAP) initiative, which builds on these principles to create an integrated suite of annual land cover and change products for the United States based on time series data from the Landsat record (i.e., Landsats 4, 5, 7, and 8). In this paper, the Landsat record refers to the time series data collected since the 1980s with the 30-m sensors of Thematic Mapper (TM), Enhanced Thematic Mapper Plus (ETM+), and Operational Land Imager (OLI). We have concentrated our efforts on Landsat data because of the long-term (> 35 years), consistent archive of visible, near-infrared, and shortwave infrared data appropriate for monitoring purposes and because the imagery has the spatial resolution (30 m) that permits the detection of land surface and land cover change at common land management scales (Roy et al., 2010). The use of all available Landsat data enables the generation of time series data sets at the temporal frequency appropriate for generating continuous land cover trends information, providing current land change information, and characterizing land surface conditions (Zhu and Woodcock, 2014; Zhu et al., 2015). The availability of infrequent land cover and land surface change information has been a major drawback in large area mapping and monitoring efforts, however, the Continuous Change Detection and Classification (CCDC) algorithm makes it feasible to generate data on land surface change with higher frequency and lower latency for land managers and scientists (Zhu and Woodcock, 2014).

After initial implementation, coding, and running the LCMAP-CCDC algorithm on selected study sites, we conducted evaluations of the resulting products across six large sites (total 540,000 km²) representing a variety of climatic and geographic settings with variable temporal patterns of change (see Fig. 1). These evaluations provided an important testing ground to assess the broad applicability of this approach for national-scale operational monitoring of land cover and condition. Our research focused on the following questions: (1) Is the CCDC monitoring approach broadly applicable and consistent across the CONUS and over a > 30-year time period? and (2) Does the use of the time series data in a repackaged Landsat archive (the Landsat Analysis Ready Data; ARD) support ease of use and consistency in detecting change on the landscape? The lessons learned from evaluating results for the six sites were used to modify the original approach and establish a robust, consistent CCDC-based methodology suitable for application at broad national scales.

2. Foundations and LCMAP methods

The foundational elements of LCMAP include a reliance on the

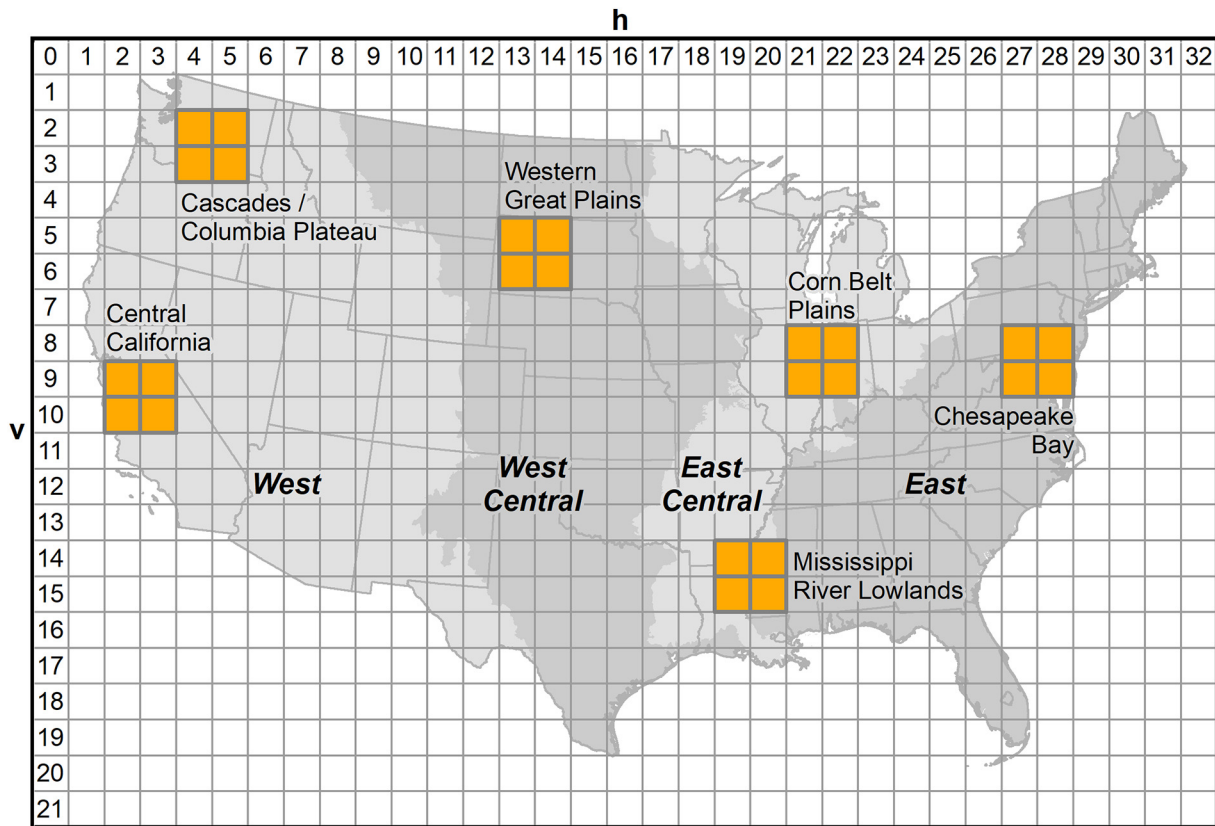


Fig. 1. Landsat ARD tiling scheme for the conterminous United States. Orange tiles delineate the location of evaluation sites used in preliminary LCMAP evaluation. The four shaded areas indicate regions for which separate accuracy assessments will be conducted. The horizontal tile number is labeled with *h*, and the vertical with *v*.

multi-decadal time series Landsat remote sensing record of the Earth's surface to perform continuous monitoring of land surface change, annual maps of land cover and land surface change with quantified accuracy and uncertainty, and statistically robust estimates of rates of land change (including land cover change and conditional change). The fundamental approach of LCMAP is to take advantage of the growing Landsat archive that is restructured into Landsat ARD by enabling efficiencies in processing, analyzing, and storing data and making data and information readily available to users. Major elements of the system described here include: (1) Landsat ARD; (2) continuous monitoring, which includes development of annual land cover and land surface change products; and (3) accuracy assessment and estimates of land cover change based on independently collected reference data (i.e., best assessment of ground condition determined independently). The resulting maps and statistical results enable improved land surface change assessments, future land cover projections, and other cyclical and special topical studies.

2.1. Analysis Ready Data

The USGS produces Landsat ARD for CONUS composed of imagery data from the TM aboard Landsats 4 and 5, Landsat 7 ETM+, and Landsat 8 OLI. These data have been processed to the highest level of geometric and radiometric quality available to produce data products suitable for use in time series analyses (USGS, 2017; Dwyer et al., 2018). The ARD provides consistent top of atmosphere at-sensor reflectance, surface reflectance, brightness temperature, and per-pixel metadata regarding data quality and provenance, gridded to an Albers Equal Area Conic projection, and tiled to 150×150 km tiles (Fig. 1).

2.2. Continuous monitoring

The LCMAP continuous monitoring capability uses all available Landsat data to characterize land surface properties through the Landsat 4–8 record, detect numerous kinds of land cover and land surface change continuously as new images are collected, and provide land cover maps for any given time. The CCDC algorithm includes two major elements, change detection and classification. The time series modeling and change detection of CCDC was based on that of Zhu et al. (2015), while the classification approach was described by Zhu et al. (2016) and Pengra et al. (2016). Annual land cover classes along with the location, timing, and other attributes of change are identified for 1985 through the present period. CCDC henceforth refers to the LCMAP implementation of the algorithm and the elements that comprise it, unless specifically stated otherwise. The LCMAP version of CCDC is available online at <https://github.com/USGS-EROS/lcmap-pyccd>.

The change detection element of CCDC utilizes all available surface reflectance measurements from Landsat ARD to estimate a time series model for the spectral response of every pixel (Eq. (1)) and to estimate the dates at which the spectral time series data diverge from past patterns. “Divergence” (referred to as a model “break”) is generally the result of an abrupt change (e.g. wildfire, logging, and land use conversions), but can also result from a gradual shift in the spectral signal (e.g., forest regrowth, insect infestation, disease, and drought). Breaks are flagged by CCDC when multiple consecutive observations are substantially different than predicted.

$$\hat{p}(i, t) = c_{0i} + c_{1i}t + \sum_{n=1}^3 \left(a_{ni} \cos \frac{2\pi nt}{T} + b_{ni} \sin \frac{2\pi nt}{T} \right) \quad (1)$$

where,

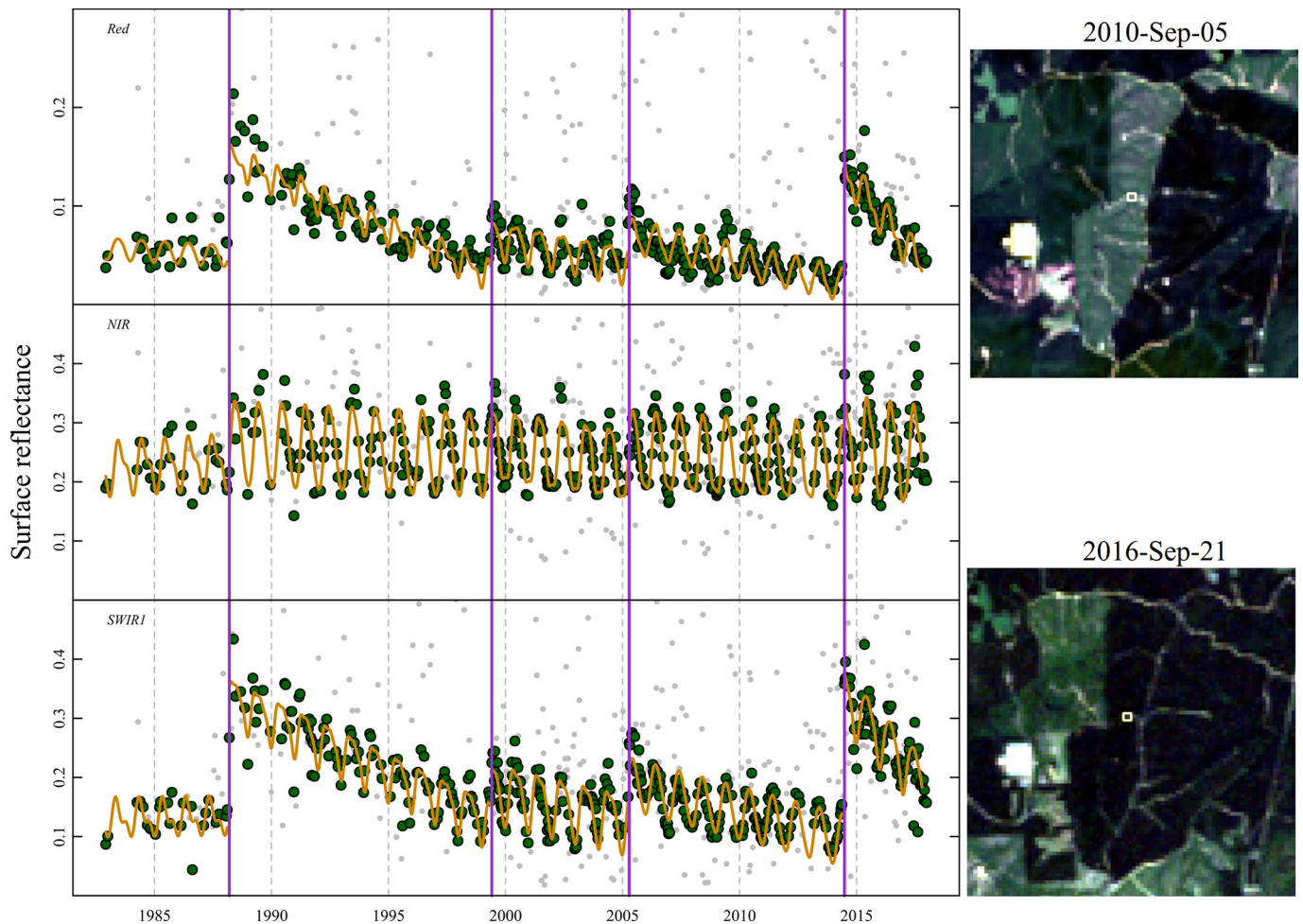


Fig. 2. Temporal profiles for a single pixel (location shown by the white box on the Landsat images to the right: true color combination). Breaks in the model, i.e., segments, are shown as purple lines. Spectral band information is for red, near-infrared, and short-wave infrared bands from Landsat 4, 5, 7, and 8 data. (For interpretation of the references to color in this figure legend, the reader is referred to the web version of this article.)

- t ordinal of the date, where January 1 of the year 1 has ordinal 1 (proleptic Gregorian calendar)
- i i th Landsat band
- T average number of days per year, 365.2425
- a_{ni} , b_{ni} estimated n th order seasonal harmonic coefficients for the i th Landsat band
- c_{0i} , c_{1i} estimated intercept and slope coefficients for the i th Landsat band
- $\hat{p}(i, t)$ predicted value for the i th Landsat band at ordinal date t

Results from CCDC change detection for a forested pixel that has undergone harvesting are illustrated in Fig. 2. In this Figure, the green dots represent the surface reflectance values from three spectral bands used to derive the actual CCDC models. Smaller gray dots represent data that were filtered out due to poor quality identified by the per-pixel data quality bands from Landsat ARD. The time series models produced by estimating the surface reflectance values are shown as orange lines. Breaks in periods with established model “segments” are designated by vertical purple lines. Major logging events occurred in 1988 and 2015, the latter of which can be seen in the Landsat images to the right of Fig. 2. Two more subtle selective thinning events in 1999 and 2005 are seen between the major logging events. For the forested pixel in this example, the spectral discontinuities are obvious in the red band and the short-wave infrared band but are not particularly apparent in the near-infrared band. Model breaks are identified by CCDC based on all Landsat channels except blue and brightness temperature.

After a break is identified, a new model is estimated.

It is worth noting that the CCDC algorithm can detect abrupt land surface changes (Zhu and Woodcock, 2014), but not all abrupt land surface changes will lead to a thematic land cover change (as defined by our classification scheme; Zhu, 2017). Although many land disturbances such as grass fires, floods, and insect infestations have ephemeral impacts on the land surface, the land cover before and after the abrupt land surface change remains the same (Zhu et al., 2019). Under certain conditions land cover thematic changes may not be caused by abrupt surface events. For some transitions in time (e.g., grass/shrub transitioning to tree cover as a clear cut regenerates to forest), no abrupt surface change occurred, but with accumulated gradual changes over a period of time (often years to decades), we observe a slower change from one land cover type to another.

The classification element of CCDC produces a land cover classification for every pixel. Unlike traditional land cover approaches, which base classification on spectral measurements, CCDC classifications are based on data from the time series models (e.g. model coefficients). In LCMAP, we generate land cover products on an annual basis for the study period. Input for CCDC classification is the output of change detection combined with ancillary data. The LCMAP land cover classification scheme is similar to that of Anderson level 1 (Anderson et al., 1976) as modified in the USGS Land Cover Trends investigations (see Table 1; Loveland et al., 2002).

Output from the two elements of CCDC are used to generate a suite of map products depicting land cover and land surface change that,

Table 1
LCMAP annual map products (version 1).

Name	Description	Attribute
Land cover products		
Primary land cover	Land cover classification consisting of eight general land cover types	Classes: developed, cropland, tree cover, grass/shrub, wetland, water, ice/snow, barren
Secondary land cover	Land cover classification consisting of eight general land cover types	Alternative cover class with the 2nd highest algorithmic probability of occurrence, same classes as primary land cover
Primary land cover confidence	A measure of confidence in the primary land cover class designation	Measure from 0 to 100; higher values imply higher levels of confidence
Secondary land cover confidence	A measure of confidence in the secondary land cover class designation	Measure from 0 to 100; higher values imply higher levels of confidence
Annual land cover change	Indicator of thematic land cover change that has occurred from the prior year to the current year (in other words, From:To land cover)	Categories that indicate two land cover states, the prior year land cover and the current year land cover
Spectral change products		
Time of spectral change	The day of year that a spectral change was detected for a given year	Data indicating location and timing of spectral model breaks
Change magnitude	A measure of the spectral magnitude of the change found within a given year	Values may be indicative of different types of spectral changes
Time since last change	The cumulative number of days since the last spectral change occurred as of July 1st of the given year	A measure of the time since a location has experienced a spectral change
Spectral stability period	A measure of the amount of time in days that a pixel has been spectrally stable	A measure of the time a location has been in its current state
Model quality	Characterization of time series model quality as it relates to model input data and model fit	A spatial measure for interpreting LCMAP product results

with independent reference data, form the basis for determining the rates and geographic extent of different dimensions of land cover and land cover changes. The independent reference data are described below, for further details see [Pengra et al., 2019](#).

2.3. LCMAP products

The CCDC approach is continuous and has the capability to identify the state of land cover and conditional surface change at any point in the Landsat temporal record. The LCMAP product suite (Version 1) includes 10 land cover and land change map products ([Table 1](#)) produced at an annual time step. These 10 products will initially be generated for 1985–2017 for the CONUS. The Version 1 annual land cover products represent the annual status of each pixel on July 1st as a representative date of each year. The land surface change products provide more information about spectral change (e.g. magnitude or date) that occurred during each annual period.

The LCMAP products provide multiple perspectives on land characteristics and changes that have occurred throughout a region through time. [Figs. 3 and 4](#) provide examples of the suite of LCMAP products listed in [Table 1](#). The Figures are for the Mount Rainier region in the state of Washington for the year 2010, with [Fig. 3](#) depicting the first four land cover products in [Table 1](#) and [Fig. 4](#) depicting LCMAP spectral change products (the last five products in [Table 1](#)). The area shown includes a portion of the Cascades, where a substantial amount of logging takes place. While the data sets depicted show information for a single year, LCMAP provides these products for every year from 1985 to present.

Primary Land Cover ([Fig. 3a](#)) is the land cover class assigned the highest probability by the CCDC classifier. That probability is reflected in the Primary Land Cover Confidence (3b) on a range of 1–100 with higher values representing higher probability, or confidence, that the assigned land cover class matches the conditions of that class represented in the training data. Secondary Land Cover (3c) represents the land cover class assigned the second highest probability by the CCDC classifier, with that probability reflected in the Secondary Land Cover Confidence (3d). In circumstances where the Primary Confidence is relatively high and the Secondary Confidence is relatively low, the Secondary Land Cover is not likely to be helpful. However, where the values of the two Confidence products begin to approach each other, the Secondary Land Cover provides the “next best” assignment of land cover, which could be associated with a classification error or provide additional information for the pixel. For example, the forested area

around Mount Rainier ([Fig. 3](#)) and the persistent snow areas at high altitude show high values in the Primary Confidence (3b) and the Secondary Land Cover (3c) does not provide additional useful information. But the transition area between the tree line and the persistent snow shows relatively lower values in the Primary Confidence and higher in the Secondary Confidence (3d). The Secondary Land Cover shows a mix of Barren, Snow/Ice, and Grass/Shrub classifications and this type of confusion is expected in those conditions. Similarly, the large patches in forested areas labeled Developed in the Secondary Land Cover have extremely low Secondary Confidence values and can be disregarded in favor of the Primary Land Cover. These examples illustrate how multiple LCMAP products used in concert can inform each other to provide increased understanding of landscape characteristics.

The Time of Spectral Change ([Fig. 4a](#)) and Change Magnitude (4b) products both represent characteristics of a “break” between two CCDC time series model segments where spectral observations diverged from the earlier model (i.e., expected spectral values or patterns). These breaks may be reflected in the Primary Land Cover between years as a change in thematic land cover or they may represent more subtle conditional surface changes that affect the spectral time series models. Time of Spectral Change provides the timing of the model break (see [Fig. 2](#)) within the product year as day-of-year. Change Magnitude provides information on the spectral strength or intensity of a model break, calculated as the magnitude of the per-band median residuals identified by CCDC. As both these products provide information about the same model breaks, they will always be coincident in time and space. The Spectral Stability Period (4c) and Time Since Last Change (4d) products both represent pixel conditions that may extend beyond the current product year. Spectral Stability Period represents the current length, in days, that the signal has been in its state. Time Since Last Change represents the time in days since the prior spectral change day and is calculated similarly, from July 1st back to the day of the most recent spectral change identified by a CCDC model break. The collective values greater than zero for Time Since Last Change in a given product year represent the to-date footprint of spectral change.

The Model Quality product ([Fig. 4e](#)) is useful for diagnosing potential areas of uncertainty and provides metadata regarding the current CCDC model for the product year. Labels of Simple, Advanced, and Full refer to the number of coefficients used in the current CCDC model (4, 6, or 8, respectively) with eight being the ideal Full model. Start Fit and End Fit labels refer to periods at the beginning and/or end of a time series, respectively, where there are insufficient data to establish a CCDC model and 4 coefficients are used. Insufficient Clear and

Fig. 3. Example of LCMAP prototype land cover products generated for 2010 for an area that includes Mount Rainier, Washington (lower left of the images) including: (a) Primary Land Cover, (b) Primary Land Cover Confidence, (c) Secondary Land Cover, and (d) Secondary Land Cover Confidence. The corresponding true-color composite derived from Landsat data is at the bottom right (e).

Persistent Snow labels refer to internal procedures within CCDC to trigger alternate methods where the full time series for a pixel has very low overall counts of “clear” observations or very high counts of “snow”, respectively, as identified by the Landsat ARD per-pixel data quality bands. A label of None in Model Quality identifies pixels that have no current model on July 1st, which likely indicates a recent CCDC model break and a gap in consistent spectral observations that would not allow establishment of a subsequent model.

2.4. Accuracy assessment, area estimation, and independent reference data

All LCMAP map products will be based on the “good practice” recommendations specified by Olofsson et al. (2014). The initial accuracy assessment objectives include determining overall, user's and producer's accuracies for the annual Primary Land Cover and Annual Land Cover Change products (Table 1). In addition, independent reference data will be used to estimate the areas of land cover and land cover change per year based on the reference classification (Olofsson et al., 2013, 2014). The methodology consists of three component protocols; the sampling design, response design, and analysis (Stehman and Czaplewski, 1998). Elements of the accuracy assessment, especially the sampling and response designs, are being done in partnership with the U.S. Forest Service Land Change Monitoring System project team (Healey et al., 2018; Pengra et al., 2019).

2.5. Evaluation methods

As part of the LCMAP prototyping process, we evaluated preliminary land cover and land surface change products calculated using Landsat ARD as input (evaluation results for the period of 1984–2015). The CCDC version used for evaluation was based on Zhu et al. (2015), Zhu et al. (2016), and Pengra et al. (2016) and differed from Version 1. We focused on six 90,000-km² evaluation sites across CONUS (Fig. 1). Each site was a 2 by 2 block of Landsat ARD tiles. The sites were chosen to represent a range of different ecoregions and patterns of land cover and land use. Goals included testing and evaluating the CCDC algorithm across a range of conditions to ensure that it could consistently quantify the 10 products listed in Table 1.

Qualitative reviews of LCMAP results were accomplished by a group of 3–8 land cover experts viewing LCMAP product data in conjunction with Google Earth imagery, Landsat imagery, land cover and land cover change data sets from NLCD and Trends, land ownership data, CCDC pixel models, fire boundaries from the Monitoring Trends in Burn Severity project (Picotte et al., 2016), and other explanatory data sets. Qualitative reviews were used to evaluate the logical and spatial consistency in the 30-year temporal sequence of land cover change. The timing of change as identified by CCDC was also evaluated via visual observation of Landsat imagery from the time series and other ancillary information (e.g., drought data, fire boundaries).

Quantitative analyses included compiling contingency tables that compared LCMAP land cover with existing Trends and NLCD land cover. The Trends and NLCD cover products were cross-walked to a classification scheme that approximates Anderson Level 1 land cover (Anderson et al., 1976) that could be compared with LCMAP. The LCMAP Primary Land Cover products were compared to Trends for the years 1992, 2000, and 2006 (where available) and to NLCD for the years 1992, 2001, 2006, and 2011. These results were used in the qualitative review sessions to further investigate areas of disagreement and identify reasons for the disagreement.

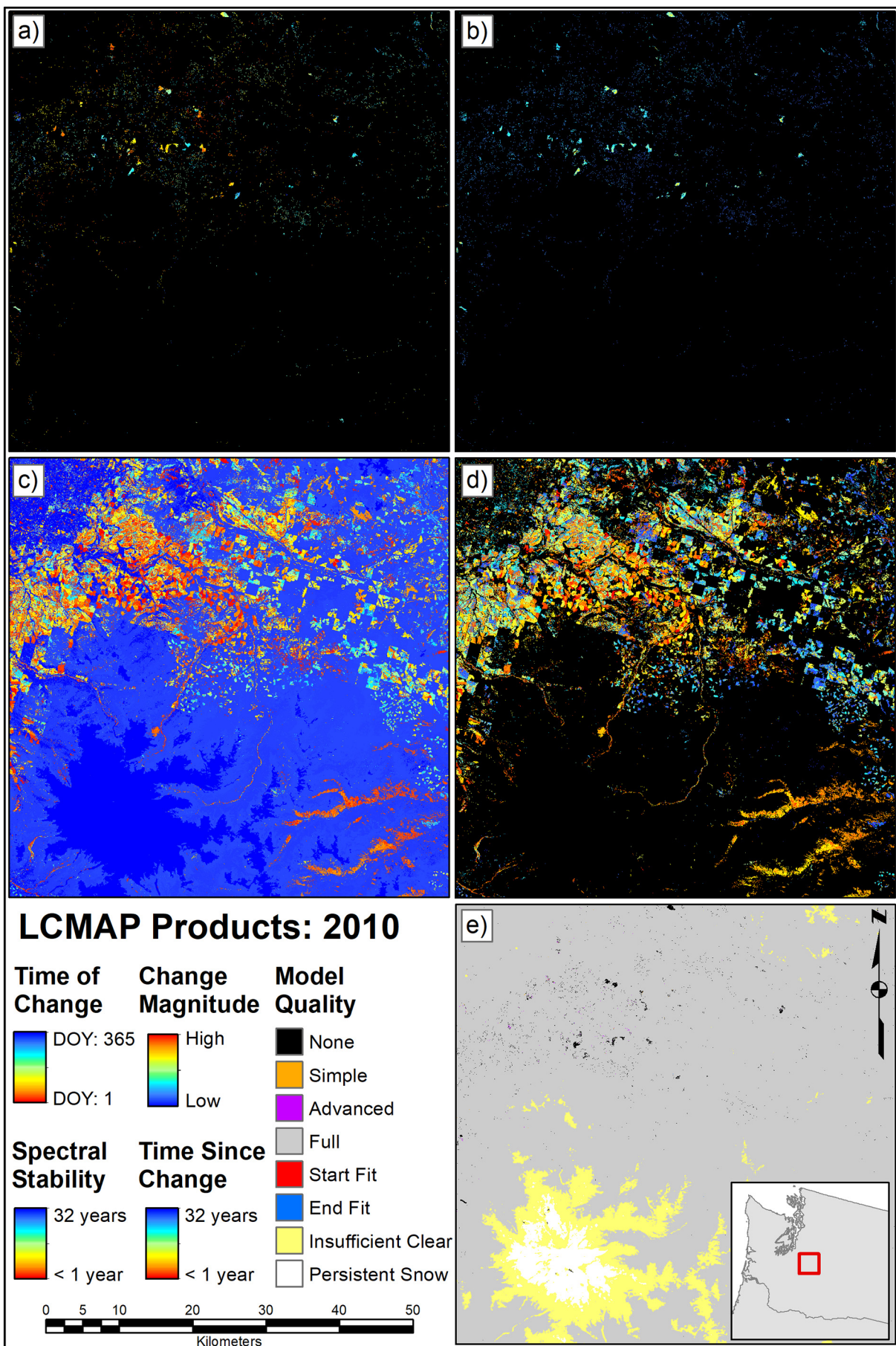
3. Results and lessons learned in implementing the LCMAP approach

3.1. Evaluation results

LCMAP land cover spatial patterns and area statistics were consistent with Trends and NLCD (Loveland et al., 2002; Homer et al., 2007; Sleeter et al., 2013; Homer et al., 2015). Evaluation results demonstrated both the power and the challenge of dense time series data over multi-decadal time spans; however, differences in observation frequency produced inconsistencies in change detection rates. Land cover evaluations also reinforced the importance of training data that represents the full range of variability seen in the study site for classification.

Initial evaluations involved quantitative inter-comparisons of our results with other known data sources on land cover and change. The LCMAP independent reference data that have been collected for validation were not utilized for initial evaluation so that their full value would be retained for accuracy assessment of Version 1 National LCMAP products. If these reference data were used for a preliminary evaluation and the LCMAP products were adjusted based on the results of the preliminary evaluation, the reference data could no longer be regarded as independent for the purposes of validating the final products. Agreement between LCMAP land cover results, Trends, and the NLCD was generally high for the dominant land cover classes for each evaluation site, although comparisons were less satisfactory for rare classes. Fig. 5 shows the similarities between Trends and LCMAP land cover and helps to demonstrate some of the strengths of LCMAP. The Trends data are the proportion of area of each class extracted from Trends sample blocks located within single tiles in selected evaluation sites. Trends consists of 2688 10 × 10 or 20 × 20 km sample blocks distributed across CONUS (covering approximately 3.7% of CONUS land area). The trend lines in Fig. 5 represent the proportion of area of LCMAP primary land cover within the same sample blocks and indicate overall patterns of temporal change occurring within those tiles. For instance, LCMAP showed a decrease in Tree Cover and increase in Developed for a portion of the Washington Cascades/Columbia Plateau during the study period. The results for Tree Cover in the uplands of the Mississippi River Lowlands contrast the Cascades results as Tree Cover in the uplands increased over the time period (at the expense of Cropland). Not only do the results summarized from annual LCMAP land cover data demonstrate the direction of the change in cover through time, they also provide more temporal detail on when changes occurred. These patterns can be related to a wide variety of factors, including different socioeconomic conditions, climatological factors, and land use history, and can help to tell a more complete temporal story of land cover change. We do not expect an exact match of the ratios of land cover within tiles between the Trends and LCMAP evaluation results as LCMAP represents continuous coverage over the entire tile and Trends is subsampled within blocks (Loveland et al., 2002).

Spectral change detection results (Fig. 4) were generally observed to be consistent with known processes that drive change. Forest clearing, fire, and development, as well as changes in water level and coverage for lakes, were usually readily discernible in the LCMAP spectral change products. Even subtle changes that may not result in a land cover (thematic) change such as selective harvesting or insect activity were observed in the LCMAP change products. Change detection was observed to be especially reliable when the time series data were relatively well-behaved and predictable (e.g., wet areas with tree cover), while areas with frequent sharp surface reflectance changes (e.g., agricultural areas) or high inter-annual variability (e.g., arid



(caption on next page)

Fig. 4. Example of LCMAP spectral change products generated for 2010 for an area that includes Mount Rainier, Washington (same area as shown in Fig. 3) including: (a) Time of Spectral Change indicated by day of year, (b) Change Magnitude, (c) Spectral Stability Period, (d) Time Since Last Change, and (e) Model Quality.

grasslands) were less consistent. In arid regions, CCDC produced frequent detection of spectral changes, particularly in Cropland and Grass/Shrub land cover. In many cases, these results could be attributed to changing weather patterns that can cause ephemeral land surface change in herbaceous vegetation and associated reflectance properties over relatively short periods of time. As expected, spectral change was relatively rare on an annual basis, but substantial over longer time periods.

Major observations from the six evaluation sites are summarized in Table 2. We observed that the CCDC approach generated unambiguous change results for some classes and for some locations, but generated results that required greater levels of interpretation and scrutiny for

others. Initial evaluations indicated that while the evaluation results were broadly useful and reasonable, some issues were noted that merited modification. An overarching goal of modifications was to make products more uniform and consistent, so that similar types of changes on the land surface are equally likely to produce a detection of change no matter where or when they occur. For land cover classification, improving consistency in the treatment of infrequent and/or highly variable classes was an important goal.

The evaluation of CCDC change and cover results across various locations in the country (Fig. 1) contributed insights into the large-scale analysis of dense time series data. While early research for CCDC was performed in a constrained geographic context (e.g. forested

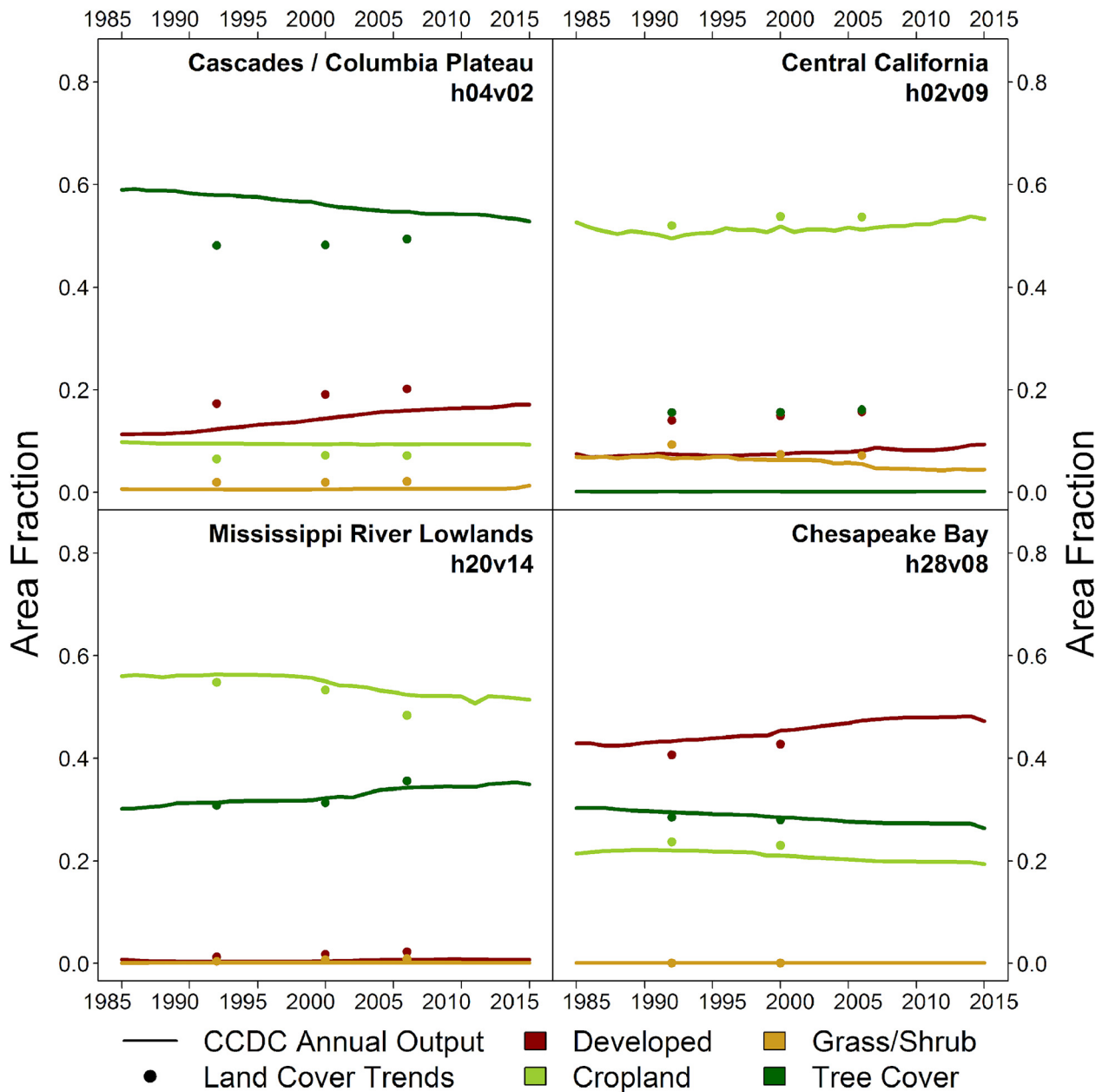


Fig. 5. Comparison between CCDC-derived Primary Land Cover class outputs and USGS Land Cover Trends data. Percent cover estimates were based on averages derived from Trends sample blocks located within four individual tiles. Vertical axes indicate the proportion of the area common to both data sets per given land cover class.

Table 2
Summary qualitative and quantitative information from study site evaluations. The overall agreement summarizes the percentage of pixels that had matching land cover labels (based on the NLCD 2011 and LCMAP results for 2011). Location of evaluation sites are shown in Fig. 1.

Evaluation site	Dominant land cover classes	Observations of note	Challenges	Percent overall agreement between LCMAP evaluation results and NLCD (2011)	Percent overall agreement between LCMAP Version 1 prototype results and NLCD (2011)
Cascades/Columbia Plateau	Tree cover, grass/shrub	Dominant land change related to logging, forest fires, and agriculture management; timing and detection of changes reflected well in LCMAP products	Classification of areas transitioning from barren to forest	80%	87%
Central California	Cropland, grass/shrub	Grass/Shrub areas characterized by high degree of variability; irrigated agriculture spectrally predictable	Many frequent changes in dry agriculture lands	75%	86%
Western Great Plains	Grass/shrub, cropland	Grass/Shrub areas spectrally variable	Highly sensitive to condition change caused by drought that is difficult to characterize; missing low-density urban features	84%	90%
Corn Belt Plains	Cropland	Cropland stable through time; Developed areas slowly expanding	Many large bright objects (e.g., buildings near cities and in country) masked out, diminishing number of useable observations	87%	90%
Mississippi River Lowlands	Tree cover, cropland, wetland	Short plantation cycles detected well (harvest, regeneration, thinning cycles); many catfish farms	Frequent cover changes in agricultural region along Mississippi River (crops, water, wetland)	73%	85%
Chesapeake Bay	Tree cover, developed, wetland, cropland, water	Developed class gradually expanding in urban corridor; coastal wetlands very stable; Time Since Last Change output very valuable in areas of sustained urbanization	Forested wetlands generally classified as Tree Cover, but secondary class in these cases generally Wetland	80%	87%

landscapes; Zhu and Woodcock, 2014; Zhu et al., 2016) using scene-based Landsat time series, LCMAP testing and evaluation of CCDC covered a larger range of environments (including rangelands, developed, and agricultural land cover). The Landsat ARD is a foundational element of LCMAP and the primary source for data. While offering characteristics that enhance its use in time series analysis, the full range of observation frequency in the Landsat record is present due to the ease of accessing every available observation on a per-pixel level, which in turn was shown to influence results. For LCMAP, the wider geographic range of test sites along with variation in observation frequency produced a wider range of results.

Many lessons learned from evaluations led to modifications in LCMAP methods that were incorporated into Version 1 products, and all provide useful context for the usage of LCMAP products and remote sensing time series analysis more broadly, highlighting differences from era- and Landsat scene-based land cover mapping. These lessons can also inform the future design and creation of time series Landsat data that are considered analysis-ready. Lessons included the importance of considering observation frequency and the subtle impacts on analysis, the importance of representative training data, and that gradual transitions need to be considered in classification.

3.2. ARD cloud detection

Cloud and snow/ice detection and masking is critical for CCDC since cloudy observations are spectrally very different from the land surface and might cause a false detection of a change if not correctly masked. The initial cloud, cloud shadow, and snow/ice masking for CCDC is derived from the per-pixel data quality flags available in Landsat ARD as PIXELQA (Dwyer et al., 2018), based on the Fmask algorithm of Zhu and Woodcock (2012). Like other cloud mask implementations, Landsat PIXELQA confuses clouds with targets that are very bright, such as metal roofs on buildings, bridges, beaches, sea foam, terrain shadow, and periodic snow/ice, and errors associated with cloud shadows (Foga et al., 2017). While these types of errors are small in area covered (from 0.1% to 2.5% of the area for our evaluation sites), these types of targets can be masked for most (or all) of the available observations in a time series. In cases where only a few observations are available in a time series, no change output is calculated (6353 pixels out of the 6×10^8 pixels in the evaluation tiles, or 0.001%).

3.3. Variability in observation frequency across space and time

A primary challenge for consistent change detection over the entire Landsat record is the variability of observation frequency across space and time. Three major sources of variability in the frequency of observations are: (1) Landsat orbital characteristics, (2) changes in data availability over time, and (3) variations in seasonal data availability due to geographical differences in snow and cloud cover.

The orbital characteristics of the Landsat satellites are the primary control of observation frequency. A single 16-day cycle of orbits for a Landsat satellite images all of CONUS at least once. Locations near the center line of the orbit track are observed once, and locations overlapped by adjacent orbits (side-lap) are observed twice. This difference is predictable over time; and with multiple sensors, for locations closest to the orbit center line and those furthest from it (maximum overlap). The location of the transitions between scene-center and side-lap areas are less predictable due to the high variability over time in orbital characteristics of Landsat 5 and Landsat 7 (Kovalskyy and Roy, 2013).

Fig. 6 shows the observation frequency throughout the data record as the number of clear observations in a 1-year period beginning with each day in the same period. Frequencies were calculated from 2000 point-sample sets, one along the down-track World Reference System-2 (WRS-2) center line and the second down the center of the WRS-2 side-lap area, across the four Landsat ARD tiles of the Cascades/Columbia Plateau study area. The most obvious changes over time are driven by

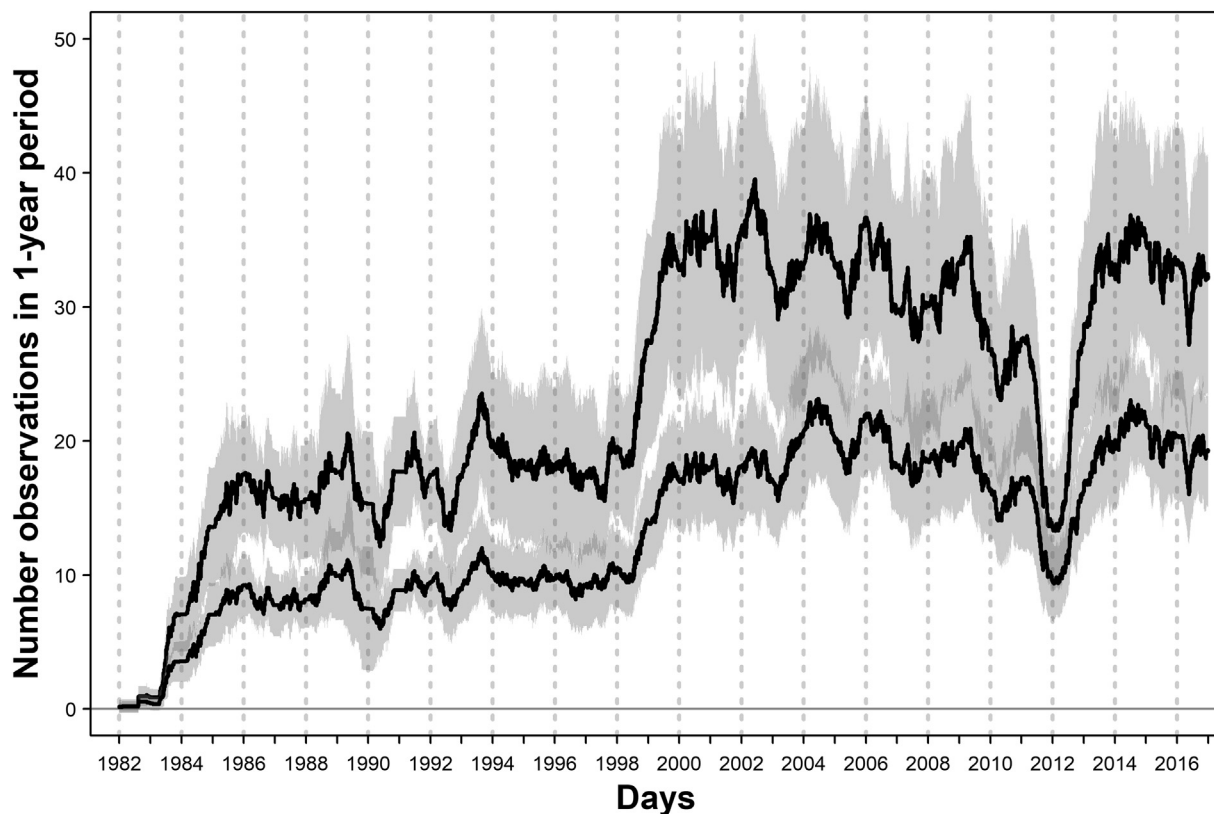


Fig. 6. Available observations in a 1-year period beginning on each day from 1982 to 2017, illustrating the differences in observation frequency near the centers of Landsat orbit tracks (bottom curve) and the World Reference System-2 (WRS-2) side-lap area (top curve). Each curve represents the mean on each day from 1000 sample points (standard deviations shaded in gray).

the inclusion of ETM+ data following the launch of Landsat 7 in 1999, the absence of TM data following the loss of Landsat 5 in 2012, and the addition of OLI data from Landsat 8 in 2013. Smaller changes can be attributed to a variety of technical, programmatic, and orbital changes over time. This variability throughout the Landsat archive has been documented previously (Markham et al., 2004; Goward et al., 2006; Loveland and Dwyer, 2012; Roy and Yan, 2018).

Seasonal variation in available observations and the differences across regional geographies is illustrated in Fig. 7. Histograms by day-of-year of all clear observations in a Landsat ARD tile (1982–2017) show the distribution of observations throughout the year. The histograms for the Central California and Cascades/Columbia Plateau areas peak from mid-summer into early fall with overall low counts of clear observations through the winter months. Conversely, the Mississippi River Lowlands and Chesapeake Bay histograms have lower peaks than the previous evaluation sites but a more consistent number of available observations across seasons. This variability is largely driven by the presence of cloud and/or snow. Acquired Landsat imagery with extremely high levels of cloud and/or snow may not meet the geodetic accuracy requirements to be included in Landsat ARD (Dwyer et al., 2018). It is also possible that acquired imagery met geodetic requirements and was included, but observations for individual pixels were identified as cloud or snow by the per-pixel data quality information.

3.4. The importance of observation frequency for change detection

A main goal for LCMAP as an operational land monitoring system is that change detection and classification algorithms operate consistently across broad U.S. geographic variability regardless of input observation quality and irregularity. This goal produces several challenges when using a temporally and spatially variable record as the source for detecting land surface change. The number of available observations

affects the frequency of changes found using the CCDC time series approach. A minimum number of consecutive observations significantly different from predicted values is required for CCDC to identify a surface change. Where many observations are available at a high frequency, only a relatively short amount of time is required to reach the required consecutive number of observations necessary for change to be identified, and hence spectral changes of shorter duration can be identified as changes when the observation frequency is high. For example, we observed differences in change detection frequency between scene-center and side-lap areas (i.e., with double the observation frequency; Fig. 8).

To reduce the impact of observation frequency and variations in the Landsat record on change detection, the number of consecutive observations CCDC required to detect change was modified. Previously, a minimum of six observations that deviated significantly from prediction were required to identify change. For Landsat, the length of time to obtain six observations ranges from 17 to 300+ days. In the modified CCDC algorithm, the number of observations required to detect change is calculated for every pixel individually by calculating the median time between two consecutive observations (t_m) across the entire time series. If t_m is < 16 days, the minimum number of observations required to detect change is scaled up by $16/t_m$ for that pixel, and the threshold that all observations need to exceed is decreased to compensate (Zhu et al., 2019). The effect of this modification was to reduce change detection frequency (especially of short-term change) in areas with high observation frequency (Fig. 8c).

Adjustment in the number of observations required to detect change on a per-pixel basis compensates for large-scale variations across space. However, temporal observation frequency effects remain a challenge. Anecdotal evidence observed during the evaluation phase provided examples of change detection omission related to wildfire under specific conditions. Fire-related change was generally detected

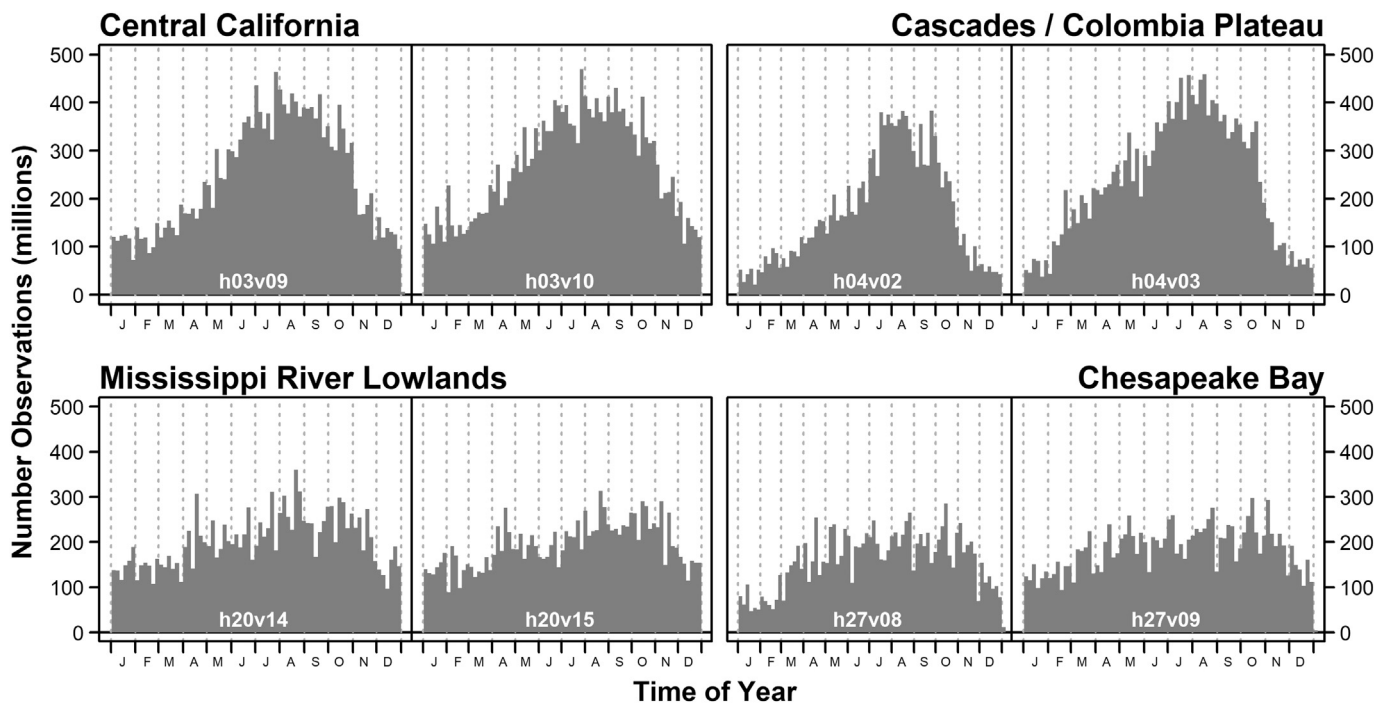


Fig. 7. Seasonal variation in available observations demonstrated with total number of clear observations in 1982–2017 (y-axis) and the day-of-year in 5-day increments (x-axis) using two illustrative examples from four of the LCMAP evaluation sites. The top examples show areas with high overall numbers of observations with the bulk of those observations in the mid to late-summer period and far fewer in the winter months. The bottom examples illustrate observations more evenly distributed throughout the year but with a lower overall total count.

consistently, but late-season grassland fires in areas receiving substantial winter snow tended to be omitted. An absence of clear observations after the first snowfall of the winter creates instances where late-season fires observed only once or twice after occurrence during the winter months do not reach the minimum number of observations to detect a change until after snowmelt in the spring – when surface reflectance often has returned to values similar to those predicted in the time series model. Additionally, large changes in frequency during the study period driven by the number of active sensors aboard Landsat satellites had an influence on the change detection record, with change detections occurring at higher rates during periods with multiple satellites in operation (e.g., from April 1999 to November 2011 while Landsats 5 and 7 were operational). Signs of these effects are apparent in the number of pixels in the evaluation areas with change detections

in each year (Fig. 9; for example, change detection frequency is lower in 2012, when there are data from only one satellite).

We observed relatively higher detection rates during drought events, which was especially conspicuous in some areas of dry-land agriculture and drought-responsive grasslands. Some locations have high inter-annual variability but do not necessarily vary much over the course of a few months. The impact of drought was less apparent in Eastern U.S. locations where drought is less frequent or severe. Drought effects were associated with high numbers of land surface changes and their meaning can be difficult to interpret. High frequency of detected changes also produced short time series models, which are prone to overfitting. The inconsistencies across large regions between swath overlap and non-overlap zones has been partially addressed with the modifications described above, but the sensitivity to detecting changes

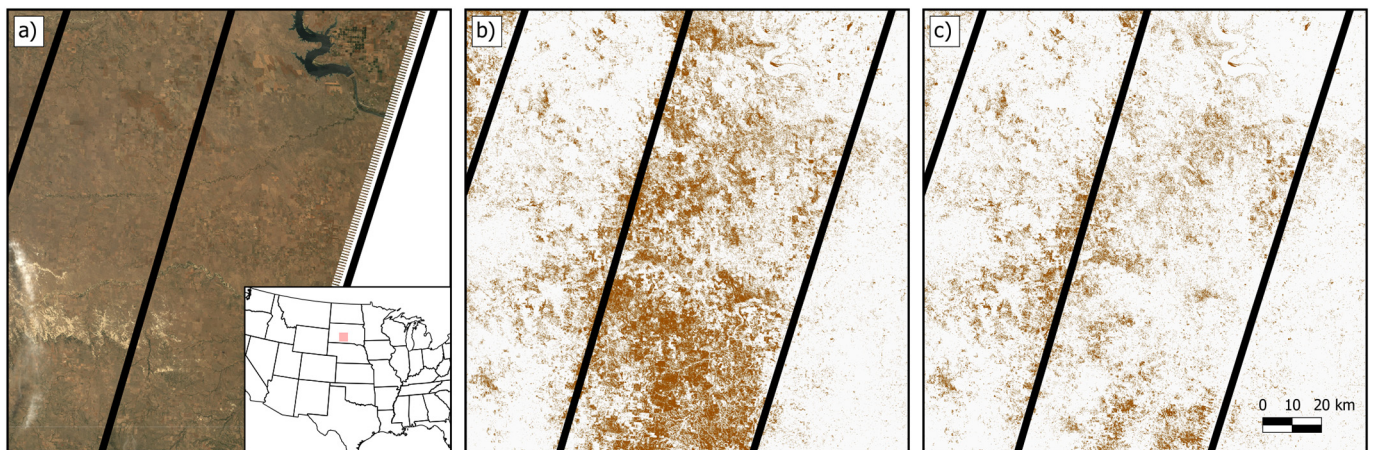


Fig. 8. Change detection results for a notable drought year (2002) in the southeast ARD tile of the Western Great Plains evaluation site (h14v06). a) A Landsat image from July 3, 2002, LT05_CU_014006_20020703_20170919_C01_V01. b) All pixels with changes detected in 2002 (dark brown) in the initial LCMAP evaluation product. c) All pixels with changes detected in 2002 in the modified LCMAP product (Version 1). Landsat swath boundaries are shown in black, with swath overlap zones in the upper left and center of the tile. (For interpretation of the references to color in this figure legend, the reader is referred to the web version of this article.)

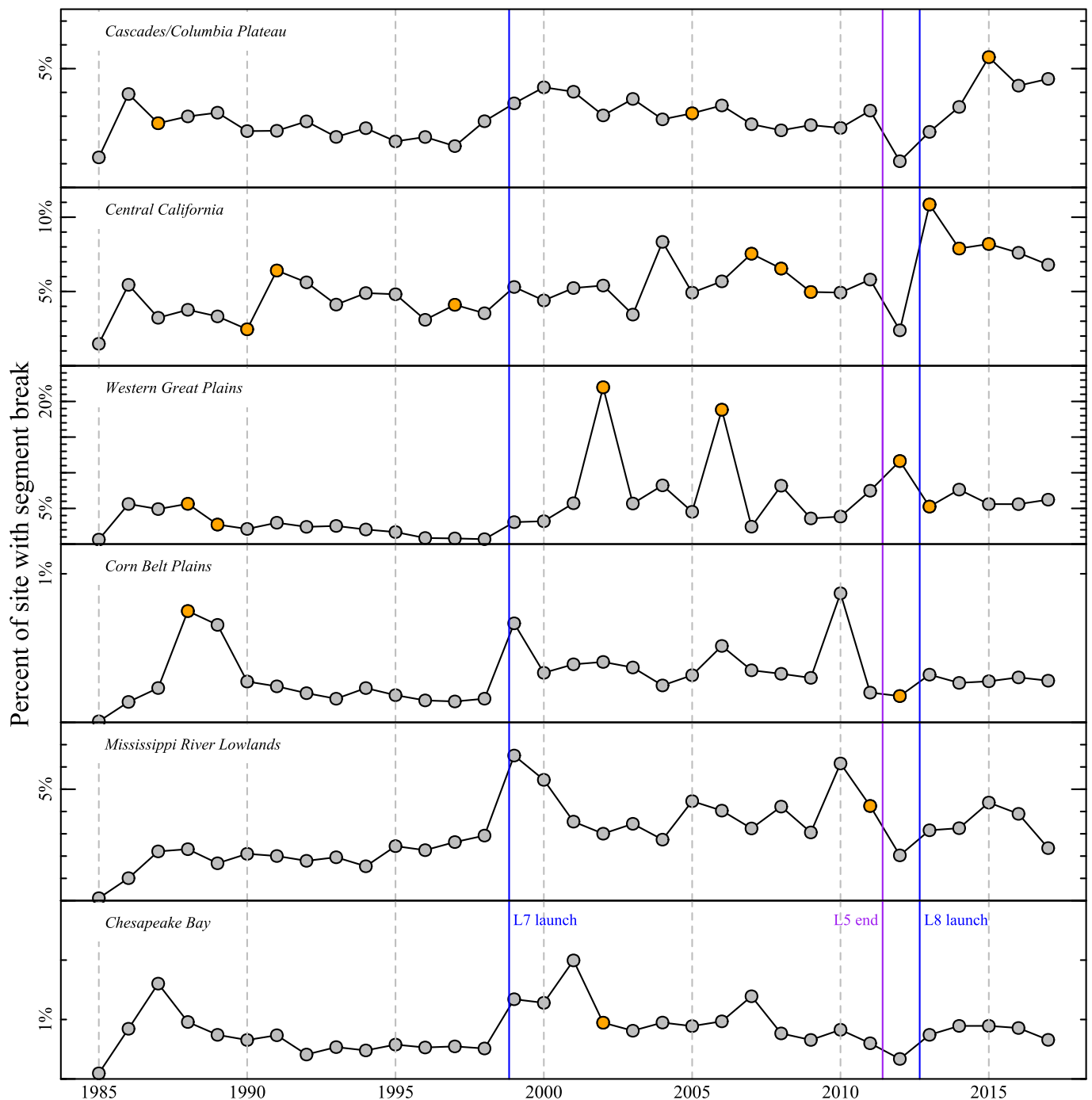


Fig. 9. Percent of evaluation site pixels with change detections (i.e. model segment breaks) in each year. Note that the y-axis scale is different for each site. Blue lines show launch dates of Landsat 7 and 8; purple is the end of TM data acquisition for Landsat 5. Orange points are years for which the majority of major climate divisions in the tile were in drought (Palmer Drought Severity Index < -4 for at least 1 month; NOAA, 2018). These results are based on the Version 1 change detection procedure. (For interpretation of the references to color in this figure legend, the reader is referred to the web version of this article.)

resulting from drought remains. Further research is needed to fully ameliorate this problem.

3.5. Monitoring gradual land cover transitions

Since the change detection element of CCDC is designed to detect abrupt changes in the land surface, land cover changes associated with these abrupt changes are well represented in the evaluation products. However, this approach does not necessarily capture more gradual and incremental land cover transitions. For example, a grass-covered

location that undergoes gradual growth of trees may not have an obvious sharp transition between Grass/Shrub and Tree Cover, and the CCDC approach often defined the entire time sequence as one model segment. In the LCMAP evaluation products, missed incremental transitions were most obvious for these Grass/Shrub to Tree Cover changes. For instance, managed forest plantations in the Mississippi River Lowlands forested areas typically are dominated by grass and shrub vegetation for a few years following harvest and then, as new trees are planted and grow, gradually transition back to dense tree cover over several years. Large areas of harvested trees with adequate time for

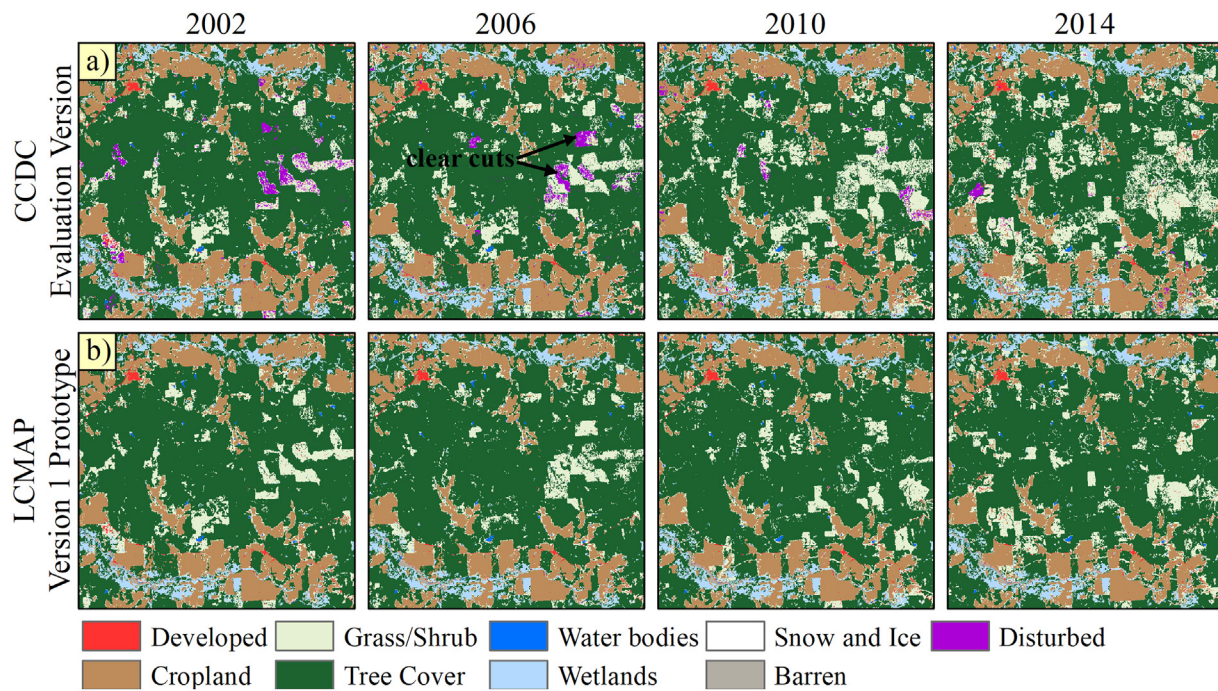


Fig. 10. Vegetation transitional increase and decrease in Mississippi Flood Plain. The “Disturbed” class in the evaluation version is defined by [Zhu et al. \(2016\)](#). a) Evaluation CCDC results show no vegetation increase over time in forest clear cuts, but b) Version 1 LCMAP prototype CCDC results show a gradual vegetation increase and transition from Grass/Shrub to Tree Cover.

regrowth remained classified as Grass/Shrub in the evaluation results ([Fig. 10](#)).

To improve classification results that better represent gradual transitions such as Grass/Shrub to Tree Cover (vegetation increase) and Tree Cover to Grass/Shrub (vegetation decrease), we classified model segment data at an annual time scale. Previously, each model segment of a time series was classified once, and the resulting land cover class was applied to the entire segment. In the modified Version 1 LCMAP method, classification is performed at July 1 for every year by including predicted per-band overall reflectance values, where overall reflectance is calculated by omitting the seasonal harmonics (see [Eq. \(1\)](#)). If the classification for a model segment is Grass/Shrub in its first year and Tree Cover in its last year, the segment is identified as experiencing increases in vegetation increase and the land cover classification for that segment is set to Grass/Shrub until the first year of Tree Cover, after which it is classified as Tree Cover. The same logic is applied to segments that have Tree Cover in the initial year and Grass/Shrub in the final year, where classification is set to Tree Cover until the first year of Grass/Shrub and Grass/Shrub after (e.g., where forest vegetation gradually decreases over multiple years). All other model segments are classified as one class per segment, determined by the class with the highest confidence for all years combined. After this modification, we were able to capture the majority of gradual transitions and did not introduce instability while classifying stable land cover classes ([Fig. 10b](#)).

3.6. A robust classification approach

Developing a robust classification methodology to generate thematic land cover on an annual basis for a large geographic region was challenging and many lessons were learned from testing and evaluation. In early research, [Zhu and Woodcock \(2014\)](#) successfully applied coefficients from the time series models and the model Root Mean Square Errors (RMSE) as classification inputs to a random forest classifier to generate annual maps for limited geographic test areas. More recently, [Zhu et al. \(2016\)](#) conducted an optimization based on 5 Landsat path/rows across the CONUS, using training data from map

products of the USGS Trends project ([Loveland et al., 2002](#)). Three of the method decisions supported by the optimization results were: (1) extracting training data based on the proportional occurrence of land cover classes with a total of 20,000 pixels, (2) balancing large and small land cover classes by using a minimum of 600 and a maximum of 8000 training pixels for each class, and (3) including eight auxiliary variables to improve classification accuracy. The auxiliary variables were based on digital elevation models (aspect, elevation, positional index, slope), ancillary data to assist in wetland detection (Wetland Potential Index), and variables based on per-pixel average quality assurance (QA) values from the PIXELQA (water probability, snow probability, and cloud probability).

LCMAP evaluations demonstrated some major issues, including: (1) misclassification of rare classes or subtypes of land cover with high internal variability (e.g., low density developed or barren) that were not represented adequately in the Trends training data and (2) Landsat 7 related Scan Line Corrector (SLC) artifacts in outputs for years prior to the launch of Landsat 7 in 1999. The first main issue (illustrated in [Fig. 11a](#)) suggested that the Trends training data set did not consistently represent within-class variability due to the Trends sampling strategy. Since Trends land cover data are available for blocks, there is the potential to entirely miss rare and/or highly variable classes. For example, while the Trends blocks include some Developed land cover in the training for the Rapid City, South Dakota tile, they do not capture substantial training data in low density developed areas (i.e., small urban centers; [Fig. 11a](#)).

The second challenge was the observation of SLC-off artifacts in pre-2003 land cover results. Because data for an entire model segment are utilized in land cover classification, data characteristics including SLC-off artifacts that exist at any time during a model segment can affect classification. Since water probability, snow probability, and cloud probability layers generated from Landsat QA values for the entire time series were used as a classification input, SLC-off artifacts were observed in LCMAP products for years before the Scan Line Corrector failure. In the modified CCDC approach, we removed these layers from the classification. We found that elimination of these layers for Version 1 reduced observations of SLC-off artifacts in land cover data.

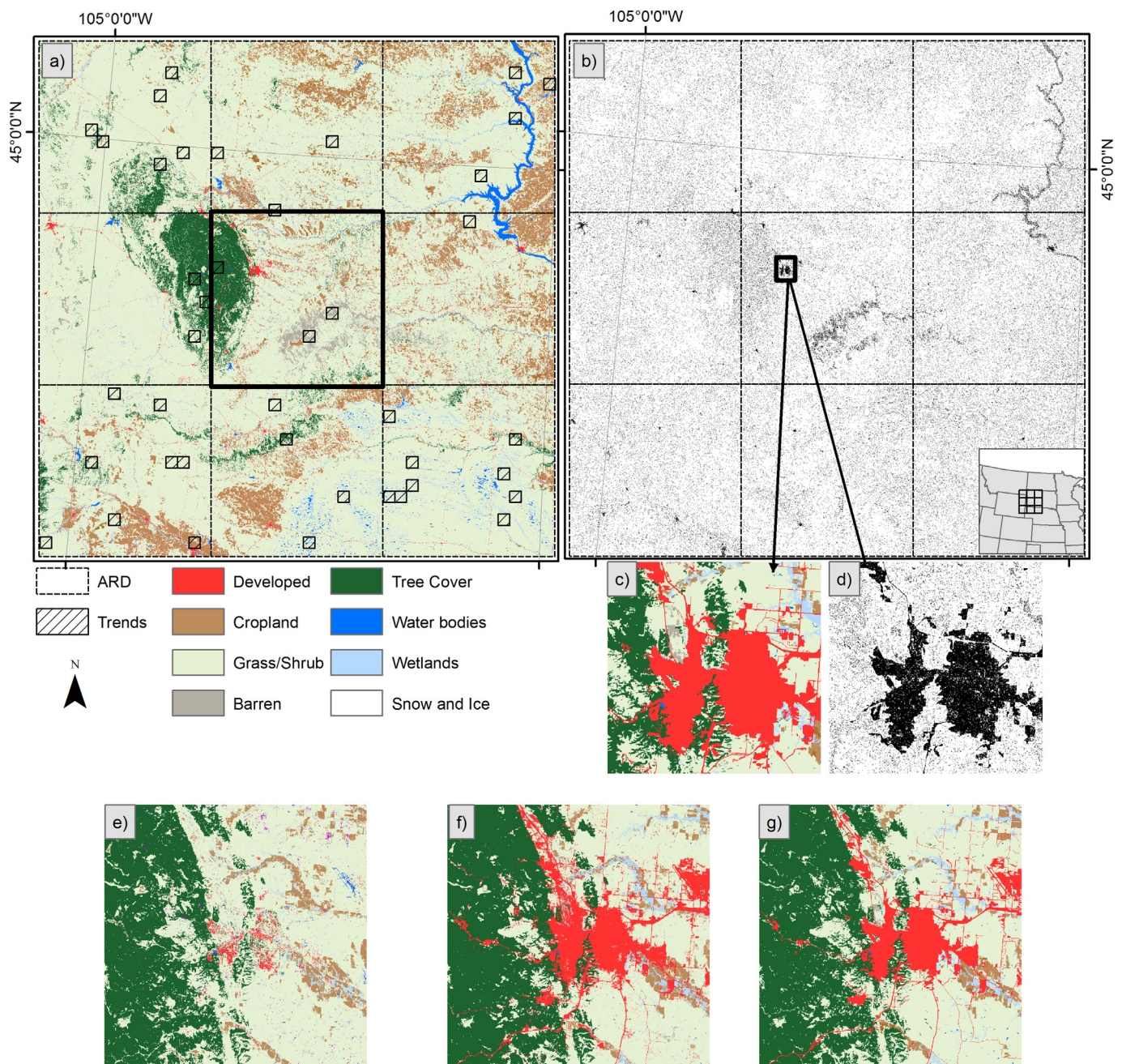


Fig. 11. LCMAP classification training data and results. a) Distribution of Trends blocks, b) distribution of the training data in black from NLCD, c) close up of Rapid City source NLCD classes, d) close up of Rapid City showing training data in black subsampled from (c), e) the initial Primary Land Cover evaluation results for 2001 using the Trends blocks as training data, f) the Version 1 LCMAP Primary Land Cover product based on training data from NLCD, and g) 2001 NLCD land cover for comparison.

We modified our strategy for LCMAP Version 1 to increase the representative training data coverage by switching from using data from Trends to NLCD (Loveland et al., 2002; Homer et al., 2007). The use of existing land cover data as an effective source for classification training has previously been demonstrated (Xian et al., 2009; Sexton et al., 2013; Radoux et al., 2014; Wessels et al., 2016; Zhang and Roy, 2017). The classification approach employs training data selected from a 3 by 3 ARD tile window where the central tile is the tile to be classified (Fig. 11), which decreases the appearance of sharp tile boundaries in land cover products. We increased to a total of 20 million training pixels based on the proportion of land cover classes and balanced larger and smaller classes by using a minimum of 600,000 and a maximum of 8,000,000 training pixels for each class. Training samples are selected

from homogeneous areas of NLCD classes, avoiding class edges to further reduce possible class confusion. The prototype Version 1 classification results show the majority of Rapid City, South Dakota, as Developed (Fig. 11f).

To reduce computation time and make the classification method operational, we replaced the random forest classifier with a boosted classification tree approach using the XGBoost software library (Chen and Guestrin, 2016). The XGBoost implementation is specifically designed for high computational performance with extremely large data sets (Chen and Guestrin, 2016). Generalization to highly variable classes from less than representative training data can also benefit from boosted classification trees over random forest (Lawrence et al., 2004; Chirici et al., 2013). Classification tree boosting has been found to

produce similar quality results to other classification approaches, including random forest, and the differences between implementations are small compared to the importance of appropriate training data (Freeman et al., 2016; Maxwell et al., 2018).

4. Conclusions

This paper describes the lessons learned and modifications made in the process of taking a research approach for continuous monitoring of land cover and land surface change into an operational setting for use in a national operational monitoring system for the conterminous United States with the goals of robust, repeatable, and geographically consistent results. The Landsat ARD is a foundation of LCMAP, but it has substantial variability in observation frequency across space and time. One of the key lessons learned was that observational frequency influences the number of changes found by CCDC, as higher observational frequency shortens the time period required for changes expressed on the landscape to be detected by multiple Landsat observations. The CCDC algorithm has been modified to minimize this problem and produce more consistent results. An algorithm modification that adjusts the requirements for consecutive observations to find change based on the frequency of observations has been implemented, and it reduces the variability in results between scene centers and scene overlap zones.

The CCDC algorithm was initially designed for monitoring abrupt changes on the land surface and has proven less effective at monitoring gradual land cover transition. The most common examples follow forest disturbances where the land cover goes through a gradual transition from Grass/Shrub to Tree Cover. When such a transition spans a single time segment as defined in the time series analysis, the original CCDC algorithm classifies the entire segment as the same class. The operational approach was modified to include both classes if the first year of the time segment and the last year of the segment switch between Grass/Shrub and Tree Cover, improving the representation of gradual changes in LCMAP results.

Classification in LCMAP was modified to improve representativeness of training data and reduce notable artifacts. First, there was misclassification of rare classes or subtypes of land cover that have high internal variability that was not represented adequately in the Trends training data. To address this problem, a dramatic change was made in the source and amount of training data used in LCMAP as well as a change in the classification algorithm. Rather than rely on the Trends data sets, which are limited to a sparse sampling of the landscape, data from NLCD were used. Since NLCD is continuous across the entire landscape, this dramatically increased available training data and minimized the problems of rare expressions of land cover types. The dramatic increase in the amount of training data led to a change from the random forest algorithm to classification using XGBoost. Second, the use of ancillary data derived from Landsat metadata led to Landsat 7 related Scan Line Corrector (SLC) artifacts in the results for years prior to the launch of Landsat 7 in 1999. This finding led to the removal of several kinds of ancillary data from the classification process.

4.1. Current status and future opportunities

Up-to-date information on LCMAP and available products can be found online (<https://usgs.gov/lcmapp/>). Version 1 LCMAP products and historical national and regional assessments of change for the lower 48 states are initially being produced for the period 1985–2017. Sample LCMAP prototype data for one California tile (h03v10; see Fig. 1) are now available (USGS, 2019) and the full Version 1 CONUS product distribution is expected in the second half of 2019. Products and assessments for Alaska and Hawaii will follow using the CCDC methodology. While the Landsat ARD data are currently available, the reference data and validation effort for Alaska and Hawaii are still under development.

Although we employed the Landsat ARD as a consistent source of

time series sensor data because the ARD is designed and processed to a high level of geometric and radiometric quality with atmospheric correction and cloud masking (Dwyer et al., 2018), opportunities exist to enhance change detection by integrating data from multiple missions. While the Landsat program is the longest running enterprise for satellite remote sensing of the Earth's land masses (Loveland and Dwyer, 2012), and as such provides data that are essential to monitor many Earth processes at the appropriate spatial scales (Townshend and Justice, 1988; Roy et al., 2010), we note that increasing the temporal frequency of observation can support community needs for intra-annual monitoring such as vegetation phenology and agricultural monitoring (Whitcraft et al., 2015; Low et al., 2018; Zhou et al., 2019). Augmenting the frequency of source observations at a similar spatial scale to Landsat sensors will likely offer further improvements to LCMAP change detection. The European Space Agency has recently launched two satellites as part of the Sentinel-2 mission (Drusch et al., 2012). Earth observations from the Sentinel-2 Multi-Spectral Instrument sensor (which collects and provides data with a similar spatial resolution to Landsat) has recently been harmonized with Landsat, supporting the effort to achieve consistent, higher frequency time series data (Claverie et al., 2018).

A future opportunity and an essential capability of the operational LCMAP system (i.e., Version 2) is the rapid detection of land change, whereby stakeholders are alerted to emerging issues or events as they occur. The CCDC is an “online” time series approach, meaning it can be updated as new observations become available. We look forward to the opportunity to use this approach to monitor change as it is occurring. Future work will be required to learn how to best provide more timely information on land cover and land surface change.

Acknowledgements

The U.S. Geological Survey supported this work through the National Land Imaging program and the Land Change Science program. Support for C. Woodcock has come from his contract (#140G0118C0006) in support of the Landsat Science Team. Support for Z. Zhu was provided under grant G17AC00057. Support for the participation of S. Stehman was provided under grant G17AC00237. Any use of trade, firm, or product names is for descriptive purposes only and does not imply endorsement by the U.S. Government.

References

- Achard, F., Eva, H.D., Mayaux, P., Stibig, H.J., Belward, A., 2004. Improved estimates of net carbon emissions from land cover change in the tropics for the 1990s. *Global Biogeochem. Cy.* 18 (12). <https://doi.org/10.1029/2003gb002142>.
- Anderson, J.R., Hardy, E.E., Roach, J.T., Witmer, R.E., 1976. A land use and land cover classification system for use with remote sensor data. In: Professional Paper 964, U.S. Geological Survey. U.S. Government Printing Office, Washington DC. <https://doi.org/10.3133/pp964>.
- Barnes, C.A., Roy, D.P., 2010. Radiative forcing over the conterminous United States due to contemporary land cover land use change and sensitivity to snow and interannual albedo variability. *J. Geophys. Res. Biogeosci.* 115, 14. <https://doi.org/10.1029/2010jg001428>.
- Brooks, E.B., Wynne, R.H., Thomas, V.A., Blinn, C.E., Coulston, J.W., 2014. On-the-fly massively multitemporal change detection using statistical quality control charts and Landsat data. *IEEE T. Geosci. Remote* 52, 3316–3332. <https://doi.org/10.1109/tgrs.2013.2272545>.
- Carpenter, S.R., DeFries, R., Dietz, T., Mooney, H.A., Polasky, S., Reid, W.V., Scholes, R.J., 2006. Millennium ecosystem assessment: research needs. *Science* 314, 257–258. <https://doi.org/10.1126/science.1131946>.
- Chen, T., Guestrin, C., 2016. XGBoost: a scalable tree boosting system. In: Proceedings of the 22nd ACM SIGKDD International Conference on Knowledge Discovery and Data Mining, San Francisco, California, USA. <https://doi.org/10.1145/2939672.2939785>.
- Chirici, G., Scotti, R., Montagni, A., Barbati, A., Cartisano, R., Lopez, G., Marchetti, M., McRoberts, R.E., Olsson, H., Corona, P., 2013. Stochastic gradient boosting classification trees for forest fuel types mapping through airborne laser scanning and IRS LISS-III imagery. *Int. J. Appl. Earth Obs. Geoinf.* 25, 87–97. <https://doi.org/10.1016/j.jag.2013.04.006>.
- Claverie, M., Ju, J., Masek, J.G., Dungan, J.L., Vermote, E.F., Roger, J.C., Skakun, S.V., Justice, C., 2018. The harmonized Landsat and Sentinel-2 surface reflectance data set. *Remote Sens. Environ.* 219, 145–161. <https://doi.org/10.1016/j.rse.2018.09.002>.

- Deng, X., Liu, J., 2012. Mapping land-cover and land-use changes in China. In: Giri, C.P. (Ed.), *Remote Sensing of Land Use and Land Cover: Principals and Applications*. CRC Press, Boca Raton, Florida, USA, pp. 339–349.
- Drusch, M., Del Bello, U., Carlier, S., Colin, O., Fernandez, V., Gascon, F., Hoersch, B., Isola, C., Laberinti, P., Martimort, P., Meygret, A., Spoto, F., Sy, O., Marchese, F., Bargellini, P., 2012. Sentinel-2: ESA's optical high-resolution mission for GMES operational services. *Remote Sens. Environ.* 120, 25–36. <https://doi.org/10.1016/j.rse.2011.11.026>.
- Dwyer, J., Roy, D., Sauer, B., Jenkerson, C., Zhang, H., Lyburner, L., 2018. Analysis Ready Data: enabling analysis of the Landsat archive. *Remote Sens.* 10, 1363. <https://doi.org/10.3390/rs10091363>.
- Eva, H., Lambin, E.F., 2000. Fires and land-cover change in the tropics: a remote sensing analysis at the landscape scale. *J. Biogeogr.* 27, 765–776. <https://doi.org/10.1046/j.1365-2699.2000.00441.x>.
- Feranec, J., Soukup, T., Hazeu, G., Jaffrain, G. (Eds.), 2016. *European Landscape Dynamics: CORINE Land Cover Data*. CRC Press, Boca Raton, Florida, USA.
- Foga, S., Scaramuzza, P.L., Guo, S., Zhu, Z., Dillej, J.R., R.D., Beckmann, T., Schmidt, G.L., Dwyer, J.L., Joseph Hughes, M., Laue, B., 2017. Cloud detection algorithm comparison and validation for operational Landsat data products. *Remote Sens. Environ.* 194, 379–390. <https://doi.org/10.1016/j.rse.2017.03.026>.
- Freeman, E.A., Moisen, G.G., Coulston, J.W., Wilson, B.T., 2016. Random forests and stochastic gradient boosting for predicting tree canopy cover: comparing tuning processes and model performance. *Can. J. For. Res.* 46, 323–339. <https://doi.org/10.1139/cjfr-2014-0562>.
- Fry, J., Xian, G.Z., Jin, S., Dewitz, J., Homer, C.G., Yang, L., Barnes, C.A., Herold, N.D., Wickham, J.D., 2011. Completion of the 2006 National Land Cover Database for the conterminous United States. *Photogramm. Eng. Rem. S.* 77, 858–864.
- Fu, P., Weng, Q.H., 2016. A time series analysis of urbanization induced land use and land cover change and its impact on land surface temperature with Landsat imagery. *Remote Sens. Environ.* 175, 205–214. <https://doi.org/10.1016/j.rse.2015.12.040>.
- Goward, S., Arvidson, T., Williams, D., Faundeen, J., Irons, J., Franks, S., 2006. Historical record of Landsat global coverage. *Mission Operations, NSLRSDA, and International Cooperator Stations*. *Photogramm. Eng. Rem. S.* 72, 1155–1169. <https://doi.org/10.14358/PERS.72.10.1155>.
- Gutman, G., Janetos, A.C., Justice, C.O., Moran, E.F., Mustard, J.F., Rindfuss, R.R., Skole, D., Turner, B.L., Cochrane, M.A. (Eds.), 2004. *Land Change Science: Observing, Monitoring and Understanding Trajectories of Change on the Earth's Surface*. Springer, Dordrecht/Boston/London, pp. 459. <https://doi.org/10.1007/978-1-4020-2562-4>.
- Hale, R.C., Gallo, K.P., Loveland, T.R., 2008. Influences of specific land use/land cover conversions on climatological normals of near-surface temperature. *J. Geophys. Res. Atmos.* 113, 9. <https://doi.org/10.1029/2007jd009548>.
- Hansen, M.C., Loveland, T.R., 2012. A review of large area monitoring of land cover change using Landsat data. *Remote Sens. Environ.* 122, 66–74. <https://doi.org/10.1016/j.rse.2011.08.024>.
- Hansen, M.C., Potapov, P.V., Moore, R., Hancher, M., Turubanova, S.A., Tyukavina, A., Thau, D., Stehman, S.V., Goetz, S.J., Loveland, T.R., Kommareddy, A., Egorov, A., Chini, L., Justice, C.O., Townshend, J.R.G., 2013. High-resolution global maps of 21st-century forest cover change. *Science* 342, 850–853. <https://doi.org/10.1126/science.1244693>.
- Hansen, M.C., Egorov, A., Potapov, P.V., Stehman, S.V., Tyukavina, A., Turubanova, S.A., Roy, D.P., Goetz, S.J., Loveland, T.R., Ju, J., Kommareddy, A., Kovalsky, V., Forsyth, C., Bents, T., 2014. Monitoring conterminous United States (CONUS) land cover change with web-enabled Landsat data (WELD). *Remote Sens. Environ.* 140, 466–484. <https://doi.org/10.1016/j.rse.2013.08.014>.
- Healey, S.P., Cohen, W.B., Yang, Z.Q., Brewer, C.K., Brooks, E.B., Gorelick, N., Hernandez, A.J., Huang, C.Q., Hughes, M.J., Kennedy, R.E., Loveland, T.R., Moisen, G.G., Schroeder, T.A., Stehman, S.V., Vogelmann, J.E., Woodcock, C.E., Yang, L.M., Zhu, Z., 2018. Mapping forest change using stacked generalization: an ensemble approach. *Remote Sens. Environ.* 204, 717–728. <https://doi.org/10.1016/j.rse.2017.09.029>.
- Hermosilla, T., Wulder, M.A., White, J.C., Coops, N.C., Hobart, G.W., 2018. Disturbance-informed annual land cover classification maps of Canada's forested ecosystems for a 29-year Landsat time series. *Can. J. Remote. Sens.* 44, 67–87. <https://doi.org/10.1080/07038992.2018.1437719>.
- Homer, C., Dewitz, J., Fry, J., Coan, M., Hossain, N., Larson, C., Herold, N., McKerrow, A., VanDriel, J.N., Wickham, J., 2007. Completion of the 2001 National Land Cover Database for the conterminous United States. *Photogramm. Eng. Rem. S.* 73, 337–341.
- Homer, C., Dewitz, J., Yang, L.M., Jin, S., Danielson, P., Xian, G., Coulston, J., Herold, N., Wickham, J., Megown, K., 2015. Completion of the 2011 National Land Cover Database for the conterminous United States - representing a decade of land cover change information. *Photogramm. Eng. Rem. S.* 81, 345–354. <https://doi.org/10.14358/pers.81.5.345>.
- Houghton, R.A., House, J.I., Pongratz, J., van der Werf, G.R., DeFries, R.S., Hansen, M.C., Le Quere, C., Ramankutty, N., 2012. Carbon emissions from land use and land-cover change. *Biogeosciences* 9, 5125–5142. <https://doi.org/10.5194/bg-9-5125-2012>.
- Hu, L., Chen, Y., Xu, Y., Zhao, Y., Yu, L., Gong, P., 2014. A 30 meter land cover mapping of China with an efficient clustering algorithm CBEST. *Sci. China Earth Sci.* 57, 2293–2304. <https://doi.org/10.1007/s11430-014-4917-1>.
- Huang, C.Q., Coward, S.N., Masek, J.G., Thomas, N., Zhu, Z.L., Vogelmann, J.E., 2010. An automated approach for reconstructing recent forest disturbance history using dense Landsat time series stacks. *Remote Sens. Environ.* 114, 183–198. <https://doi.org/10.1016/j.rse.2009.08.017>.
- Hughes, M.J., Kaylor, S.D., Hayes, D.J., 2017. Patch-based forest change detection from Landsat time series. *Forests* 8 (22). <https://doi.org/10.3390/f8050166>.
- IBGE, Instituto Brasileiro de Geografia e Estatística, 2018. *Monitoramento da cobertura e uso da terra do Brasil*. IBGE, Rio de Janeiro, pp. 2014–2016.
- Inglada, J., Vincent, A., Arias, M., Tardy, B., Morin, D., Rodes, I., 2017. Operational high resolution land cover map production at the country scale using satellite image time series. *Remote Sens.* 9, 95. <https://doi.org/10.3390/rs9010095>.
- INPE, Instituto Nacional de Pesquisas Espaciais, 2018. *Projeto Prodes: Monitoramento da Floresta Amazônica Brasileira por satélite*. Available online at: <http://www.obt.inpe.br/OBT/assuntos/programas/amazonia/prodes>, Accessed date: 24 May 2019.
- Kennedy, R.E., Yang, Z.G., Cohen, W.B., 2010. Detecting trends in forest disturbance and recovery using yearly Landsat time series: 1. LandTrendr - temporal segmentation algorithms. *Remote Sens. Environ.* 114, 2897–2910. <https://doi.org/10.1016/j.rse.2010.07.008>.
- Kennedy, R.E., Andrefouet, S., Cohen, W.B., Gomez, C., Griffiths, P., Hais, M., Healey, S.P., Helmer, E.H., Hostert, P., Lyons, M.B., Meigs, G.W., Pflugmacher, D., Phinn, S.R., Powell, S.L., Scarth, P., Sen, S., Schroeder, T.A., Schneider, A., Sonnenschein, R., Vogelmann, J.E., Wulder, M.A., Zhu, Z., 2014. Bringing an ecological view of change to Landsat-based remote sensing. *Front. Ecol. Environ.* 12, 339–346. <https://doi.org/10.1890/150666>.
- Kovalsky, V., Roy, D.P., 2013. The global availability of Landsat 5 TM and Landsat 7 ETM+ land surface observations and implications for global 30m Landsat data product generation. *Remote Sens. Environ.* 130, 280–293. <https://doi.org/10.1016/j.rse.2012.12.003>.
- Latifovic, R., Pouliot, D., 2005. Multitemporal land cover mapping for Canada: methodology and products. *Can. J. Remote. Sens.* 31, 347–363. <https://doi.org/10.5589/m05-019>.
- Lawrence, R., Bunn, A., Powell, S., Zambon, M., 2004. Classification of remotely sensed imagery using stochastic gradient boosting as a refinement of classification tree analysis. *Remote Sens. Environ.* 90, 331–336. <https://doi.org/10.1016/j.rse.2004.01.007>.
- Li, X.C., Zhou, Y.Y., Asrar, G.R., Mao, J.F., Li, X.M., Li, W.Y., 2017. Response of vegetation phenology to urbanization in the conterminous United States. *Glob. Change Biol.* 23, 2818–2830. <https://doi.org/10.1111/gcb.13562>.
- Liu, S.G., Loveland, T.R., Kurtz, R.M., 2004. Contemporary carbon dynamics in terrestrial ecosystems in the southeastern plains of the United States. *Environ. Manag.* 33, S442–S456. <https://doi.org/10.1007/s00267-003-9152-z>.
- Loveland, T.R., Dwyer, J.L., 2012. Landsat: building a strong future. *Remote Sens. Environ.* 122, 22–29. <https://doi.org/10.1016/j.rse.2011.09.022>.
- Loveland, T.R., Sohl, T.L., Stehman, S.V., Gallant, A.L., Saylor, K.L., Napton, D.E., 2002. *A strategy for estimating the rates of recent United States land-cover changes*. *Photogramm. Eng. Rem. S.* 68, 1091–1099.
- Low, F., Biradar, C., Dubovyk, O., Fliemann, E., Akramkhanov, A., Vallejo, A.N., Waldner, F., 2018. Regional-scale monitoring of cropland intensity and productivity with multi-source satellite image time series. *GIScience and Remote Sensing* 55, 539–567. <https://doi.org/10.1080/15481603.2017.1414010>.
- Lyburner, L., Tan, P., McIntyre, A., Lewis, A., Thankappan, M., 2013. Dynamic land cover dataset version 2: 2001-now...a land cover odyssey. In: *Proceedings of the 2013 IEEE International Geoscience and Remote Sensing Symposium-IGARSS*, Melbourne, Victoria, Australia. <https://doi.org/10.1109/IGARSS.2013.6723532>.
- Macedo, R., Z. Moreira, M., Domingues, E., M. R. C. Gama, A., E. G. Sanson, F., W. Teixeira, F., P. Dias, F., Yamaguchi, F., and Jacintho, R., 2013. LUCC (land use and cover change) and the environmental-economic accounts system in Brazil. *J. of Earth Sci. Eng.*, 3, 840–844.
- Markham, B.L., Storey, J.C., Williams, D.L., Irons, J.R., 2004. Landsat sensor performance: history and current status. *IEEE T. Geosci. Remote* 42, 2691–2694. <https://doi.org/10.1109/TGRS.2004.840720>.
- Masek, J.G., Huang, C.Q., Wolfe, R., Cohen, W., Hall, F., Kutler, J., Nelson, P., 2008. North American forest disturbance mapped from a decadal Landsat record. *Remote Sens. Environ.* 112, 2914–2926. <https://doi.org/10.1016/j.rse.2008.02.010>.
- Maxwell, A.E., Warner, T.A., Fang, F., 2018. Implementation of machine-learning classification in remote sensing: an applied review. *Int. J. Remote Sens.* 39, 2784–2817. <https://doi.org/10.1080/01431161.2018.1433343>.
- Melaas, E.K., Friedl, M.A., Zhu, Z., 2013. Detecting interannual variation in deciduous broadleaf forest phenology using Landsat TM/ETM plus data. *Remote Sens. Environ.* 132, 176–185. <https://doi.org/10.1016/j.rse.2013.01.011>.
- National Research Council, 2001. *Grand Challenges in Environmental Sciences*. The National Academy Press, Washington, DC. <https://doi.org/10.17226/9975>.
- NOAA, National Oceanic and Atmospheric Administration, 2018. On-line data at: <https://www1.nce.noaa.gov/pub/data/cirs/climdiv/climdiv-pdsdiv-v1.0.0-20180806>, Accessed date: 17 August 2018.
- Olofsson, P., Foody, G.M., Stehman, S.V., Woodcock, C.E., 2013. Making better use of accuracy data in land change studies: estimating accuracy and area and quantifying uncertainty using stratified estimation. *Remote Sens. Environ.* 129, 122–131. <https://doi.org/10.1016/j.rse.2012.10.031>.
- Olofsson, P., Foody, G.M., Herold, M., Stehman, S.V., Woodcock, C.E., Wulder, M.A., 2014. Good practices for estimating area and assessing accuracy of land change. *Remote Sens. Environ.* 148, 42–57. <https://doi.org/10.1016/j.rse.2014.02.015>.
- Olthoff, I., Latifovic, R., Pouliot, D., 2015. Medium resolution land cover mapping of Canada from SPOT 4/5 data. In: *Geomatics Canada, Open File 4*, <https://doi.org/10.4095/295751>.
- Pengra, B., Gallant, A.L., Zhu, Z., Dahal, D., 2016. Evaluation of the initial thematic output from a continuous change-detection algorithm for use in automated operational land-change mapping by the US Geological Survey. *Remote Sens.* 8 (33). <https://doi.org/10.3390/rs8100811>.
- Pengra, B.W., Stehman, S.V., Horton, J.A., Dockter, D.J., Schroeder, T.A., Yang, Z., Cohen, W.B., Healey, S.P., Loveland, T.R., 2019. Quality control and assessment of interpreter consistency of annual land cover reference data in an operational national

- monitoring program. *Remote Sens. Environ.* <https://doi.org/10.1016/j.rse.2019.111261>.
- Picotte, J.J., Peterson, B., Meier, G., Howard, S.M., 2016. 1984–2010 trends in fire burn severity and area for the conterminous US. *Int. J. Wildland Fire* 25, 413–420. <https://doi.org/10.1071/wf15039>.
- Radoux, J., Lamarche, C., Van Bogaert, E., Bontemps, S., Brockmann, C., Defourny, P., 2014. Automated training sample extraction for global land cover mapping. *Remote Sens.* 6, 3965–3987. <https://doi.org/10.3390/rs6053965>.
- Rollins, M.G., 2009. LANDFIRE: a nationally consistent vegetation, wildland fire, and fuel assessment. *Int. J. Wildland Fire* 18, 235–249. <https://doi.org/10.1071/wf08088>.
- Roy, D.P., Yan, L., 2018. Robust Landsat-based crop time series modelling. *Remote Sens. Environ.* <https://doi.org/10.1016/j.rse.2018.06.038>.
- Roy, P., Murthy, M., Sharma, J., Murthy, Y.V.S., Veena Suresh, S., Murthy, K.S., Kandrika, S., Kameswara Rao, S.V.C., Anasuya, T., Porwal, M.C., Pathak, S., Ravi Kumar, M.V., Bothale, V., Sekhar, N.S., Ramadevi, D., James, L., Satyanarayana, P., Fyze, M., Wadodkar, M., Debnath, B., 2008. Technical report on national land use and land cover (LULC) mapping using multi-temporal AWiFS data: interim report of fourth cycle (2007–08) and change analysis of 4 cycles. In: Technical Report NRSC/RS&GIS/JAN'09/TR-30. India, National Remote Sensing Centre, Hyderabad.
- Roy, D.P., Ju, J., Kline, K., Scaramuzza, P.L., Kovalsky, V., Hansen, M., Loveland, T.R., Vermote, E., Zhang, C., 2010. Web-enabled Landsat data (WELD): Landsat ETM+ composited mosaics of the conterminous United States. *Remote Sens. Environ.* 114, 35–49. <https://doi.org/10.1016/j.rse.2009.08.011>.
- Schepaschenko, D., McCallum, I., Shvidenko, A., Fritz, S., Kraxner, F., Obersteiner, M., 2011. A new hybrid land cover dataset for Russia: a methodology for integrating statistics, remote sensing and in situ information. *J. Land Use Sci.* 6, 245–259. <https://doi.org/10.1080/1747423X.2010.511681>.
- Senay, G.B., Friedrichs, M., Singh, R.K., Velpuri, N.M., 2016. Evaluating Landsat 8 evapotranspiration for water use mapping in the Colorado River basin. *Remote Sens. Environ.* 185, 171–185. <https://doi.org/10.1016/j.rse.2015.12.043>.
- Sexton, J.O., Song, X.P., Feng, M., Noojipady, P., Anand, A., Huang, C.Q., Kim, D.H., Collins, K.M., Channan, S., DiMiceli, C., Townshend, J.R., 2013. 30-m resolution continuous fields of tree cover: Landsat-based rescaling of MODIS vegetation continuous fields with LiDAR-based estimates of error. *Int. J. Digit. Earth* 6, 427–448. <https://doi.org/10.1080/10.1080/17538947.2013.786146>.
- Sleeter, B.M., Sohl, T.L., Bouchard, M.A., Reker, R.R., Soular, C.E., Acevedo, W., Griffith, G.E., Sleeter, R.R., Auch, R.F., Saylor, K.L., Prisle, S., Zhu, Z.L., 2012. Scenarios of land use and land cover change in the conterminous United States: utilizing the special report on emission scenarios at ecoregional scales. *Global Environ. Chang.* 22, 896–914. <https://doi.org/10.1016/j.gloenvcha.2012.03.008>.
- Sleeter, B.M., Sohl, T.L., Loveland, T.R., Auch, R.F., Acevedo, W., Drummond, M.A., Saylor, K.L., Stehman, S.V., 2013. Land-cover change in the conterminous United States from 1973 to 2000. *Global Environ. Chang.* 23, 733–748. <https://doi.org/10.1016/j.gloenvcha.2013.03.006>.
- Sohl, T.L., Sleeter, B.M., Saylor, K.L., Bouchard, M.A., Reker, R.R., Bennett, S.L., Sleeter, R.R., Kanengieter, R.L., Zhu, Z.L., 2012. Spatially explicit land-use and land-cover scenarios for the Great Plains of the United States. *Agric. Ecosyst. Environ.* 153, 1–15. <https://doi.org/10.1016/j.agee.2012.02.019>.
- Sohl, T., Reker, R., Bouchard, M., Saylor, K., Dornbierer, J., Wika, S., Quenzer, R., Friesz, A., 2016. Modeled historical land use and land cover for the conterminous United States. *J. Land Use Sci.* 11, 476–499. <https://doi.org/10.1080/1747423x.2016.1147619>.
- Song, X.P., Hansen, M.C., Stehman, S.V., Potapov, P.V., Tyukavina, A., Vermote, E.F., Townshend, J.R., 2018. Global land change from 1982 to 2016. *Nature* 560, 639–643. <https://doi.org/10.1038/s41586-018-0411-9>.
- Soulard, C.E., Wilson, T.S., 2015. Recent land-use/land-cover change in the Central California Valley. *J. Land Use Sci.* 10, 59–80. <https://doi.org/10.1080/1747423X.2013.841297>.
- Stehman, S.V., Czaplewski, R.L., 1998. Design and analysis for thematic map accuracy assessment: fundamental principles. *Remote Sens. Environ.* 64, 331–344. [https://doi.org/10.1016/s0034-4257\(98\)00010-8](https://doi.org/10.1016/s0034-4257(98)00010-8).
- Stow, D.A., Hope, A., McGuire, D., Verbyla, D., Gamon, J., Huemmrich, F., Houston, S., Racine, C., Sturm, M., Tape, K., Hinzman, L., Yoshikawa, K., Tweedie, C., Noyle, B., Silapaswan, C., Douglas, D., Griffith, B., Jia, G., Epstein, H., Walker, D., Daeschner, S., Petersen, A., Zhou, L.M., Myneni, R., 2004. Remote sensing of vegetation and land-cover change in arctic tundra ecosystems. *Remote Sens. Environ.* 89, 281–308. <https://doi.org/10.1016/j.rse.2003.10.018>.
- Tan, Z.X., Liu, S.G., Sohl, T.L., Wu, Y.P., Young, C.J., 2015. Ecosystem carbon stocks and sequestration potential of federal lands across the conterminous United States. *P. Natl. Acad. Sci. USA* 112, 12723–12728. <https://doi.org/10.1073/pnas.1512542112>.
- Townshend, J.R.G., Justice, C.O., 1988. Selecting the spatial-resolution of satellite sensors required for global monitoring of land transformations. *Int. J. Remote Sens.* 9, 187–236. <https://doi.org/10.1080/01431168808954847>.
- Turner, B.L., Lambin, E.F., Reenberg, A., 2007. The emergence of land change science for global environmental change and sustainability. *P. Natl. Acad. Sci. USA* 104, 20666–20671. <https://doi.org/10.1073/pnas.0704119104>.
- USGS, U.S. Geological Survey, 2017. U.S. Landsat Analysis Ready Data (ARD) Level-2 Data Product. <https://doi.org/10.5066/F7319TJ>.
- USGS, U.S. Geological Survey, 2019. Sample LCMAP Science Product Suite. Available online at: <https://www.usgs.gov/land-resources/eros/lcmmap/lcmmap-sample-products>, Last accessed May 8, 2019, <https://doi.org/10.5066/P9JZ5YYB>.
- Verbesselt, J., Zeileis, A., Herold, M., 2012. Near real-time disturbance detection using satellite image time series. *Remote Sens. Environ.* 123, 98–108. <https://doi.org/10.1016/j.rse.2012.02.022>.
- Vogelmann, J.E., Sohl, T.L., Howard, S.M., 1998. Regional characterization of land cover using multiple sources of data. *Photogramm. Eng. Rem. S.* 64, 45–57.
- Vogelmann, J.E., Xian, G., Homer, C., Tolck, B., 2012. Monitoring gradual ecosystem change using Landsat time series analyses: case studies in selected forest and rangeland ecosystems. *Remote Sens. Environ.* 122, 92–105. <https://doi.org/10.1016/j.rse.2011.06.027>.
- Wessels, K.J., van den Bergh, F., Roy, D.P., Salmon, B.P., Steenkamp, K.C., MacAlister, B., Swanepoel, D., Jewitt, D., 2016. Rapid land cover map updates using change detection and robust random forest classifiers. *Remote Sens.* 8 (24). <https://doi.org/10.3390/rs8110888>.
- Whitcraft, A.K., Becker-Reshef, I., Killough, B.D., Justice, C.O., 2015. Meeting earth observation requirements for global agricultural monitoring: an evaluation of the revisit capabilities of current and planned moderate resolution optical earth observing missions. *Remote Sens.* 7, 1482–1503. <https://doi.org/10.3390/rs70201482>.
- Wu, Y.P., Liu, S.G., Tan, Z.X., 2015. Quantitative attribution of major driving forces on soil organic carbon dynamics. *J. Adv. Model. Earth Sy.* 7, 21–34. <https://doi.org/10.1002/2014ms000361>.
- Wulder, M.A., Coops, N.C., Roy, D.P., White, J.C., Hermosilla, T., 2018. Land cover 2.0. *Int. J. Remote Sens.* 39, 4254–4284. <https://doi.org/10.1080/01431161.2018.1452075>.
- Xian, G., Homer, C., Fry, J., 2009. Updating the 2001 National Land Cover Database land cover classification to 2006 by using Landsat imagery change detection methods. *Remote Sens. Environ.* 113, 1133–1147. <https://doi.org/10.1016/j.rse.2009.02.004>.
- Xian, G., Homer, C., Demitz, J., Fry, J., Hossain, N., Wickham, J., 2011. Change of impervious surface area between 2001 and 2006 in the conterminous United States. *Photogramm. Eng. Rem. S.* 77, 758–762.
- Yan, W.Y., Shaker, A., El-Ashmary, N., 2015. Urban land cover classification using airborne LiDAR data: a review. *Remote Sens. Environ.* 158, 295–310. <https://doi.org/10.1016/j.rse.2014.11.001>.
- Zhang, H.K., Roy, D.P., 2017. Using the 500m MODIS land cover product to derive a consistent continental scale 30m Landsat land cover classification. *Remote Sens. Environ.* 197, 15–34. <https://doi.org/10.1016/j.rse.2017.05.024>.
- Zhou, D.C., Zhao, S.Q., Zhang, L.X., Liu, S.G., 2016. Remotely sensed assessment of urbanization effects on vegetation phenology in China's 32 major cities. *Remote Sens. Environ.* 176, 272–281. <https://doi.org/10.1016/j.rse.2016.02.010>.
- Zhou, Q., Rover, J., Brown, J., Worstell, B., Howard, D., Wu, Z.T., Gallant, A.L., Rundquist, B., Burke, M., 2019. Monitoring landscape dynamics in central US grasslands with harmonized Landsat-8 and Sentinel-2 time series data. *Remote Sens.* 11 (23). <https://doi.org/10.3390/rs11030328>.
- Zhu, Z., 2017. Change detection using Landsat time series: a review of frequencies, pre-processing, algorithms, and applications. *ISPRS J. Photogramm. Remote Sens.* 130, 370–384. <https://doi.org/10.1016/j.isprsjprs.2017.06.013>.
- Zhu, Z., Woodcock, C.E., 2012. Object-based cloud and cloud shadow detection in Landsat imagery. *Remote Sens. Environ.* 118, 83–94. <https://doi.org/10.1016/j.rse.2011.10.028>.
- Zhu, Z., Woodcock, C.E., 2014. Continuous change detection and classification of land cover using all available Landsat data. *Remote Sens. Environ.* 144, 152–171. <https://doi.org/10.1016/j.rse.2014.01.011>.
- Zhu, Z., Woodcock, C.E., Holden, C., Yang, Z.Q., 2015. Generating synthetic Landsat images based on all available Landsat data: predicting Landsat surface reflectance at any given time. *Remote Sens. Environ.* 162, 67–83. <https://doi.org/10.1016/j.rse.2015.02.009>.
- Zhu, Z., Gallant, A.L., Woodcock, C.E., Pengra, B., Olofsson, P., Loveland, T.R., Jin, S., Dahal, D., Yang, L., Auch, R.F., 2016. Optimizing selection of training and auxiliary data for operational land cover classification for the LCMAP initiative. *ISPRS J. Photogramm. Remote Sens.* 122, 206–221. <https://doi.org/10.1016/j.isprsjprs.2016.11.004>.
- Zhu, Z., Zhang, J., Yang, Z., Aljaddani, A.H., Cohen, W.B., Qiu, S., Zhou, C., 2019. Continuous monitoring of land disturbance based on Landsat time series. *Remote Sens. Environ.* <https://doi.org/10.1016/j.rse.2019.03.009>.